

HELIUM-CORE WHITE DWARFS IN THE GLOBULAR CLUSTER NGC 6397

RACHEL R. STRICKLER^{1,2}, ADRIENNE M. COOL², JAY ANDERSON³, HALDAN N. COHN⁴, PHYLLIS M. LUGGER⁴, ALDO M. SERENELLI⁵

OCTOBER 23, 2018

Draft version October 23, 2018

ABSTRACT

We present results of a study of the central regions of NGC 6397 using Hubble Space Telescope’s Advanced Camera for Surveys (HST ACS), focusing on a group of 24 faint blue stars that form a sequence parallel to, but brighter than, the more populated sequence of carbon-oxygen white dwarfs (CO WDs). Using F625W, F435W, and F658N filters with the Wide Field Channel (WFC) we show that these stars, 18 of which are newly discovered, have magnitudes and colors consistent with those of helium-core white dwarfs (He WDs) with masses $\sim 0.2 - 0.3M_{\odot}$. Their $H\alpha - R_{625}$ colors indicate that they have strong $H\alpha$ absorption lines, which distinguishes them from cataclysmic variables in the cluster. The radial distribution of the He WDs is significantly more concentrated to the cluster center than that of either the CO WDs or the turnoff stars and most closely resembles that of the cluster’s blue stragglers. Binary companions are required to explain the implied dynamical masses. We show that the companions cannot be main-sequence stars and are most likely heavy CO WDs. The number and photometric masses of the observed He WDs can be understood if $\sim 1 - 5\%$ of the main-sequence stars within the half-mass radius of the cluster have white dwarf companions with orbital periods in the range $\sim 1 - 20$ days at the time they reach the turnoff. In contrast to the CO WD sequence, the He WD sequence comes to an end at $R_{625} \simeq 24.5$, well above the magnitude limit of the observations. We explore the significance of this finding in the context of thick vs. thin hydrogen envelope models and compare our results to existing theoretical predictions. In addition, we find strong evidence that the vast majority of the CO WDs in NGC 6397 down to $T_{eff} \simeq 10,000$ K are of the DA class. Finally, we use the CO WD sequence together with theoretical cooling models to measure a distance to the cluster of 2.34 ± 0.13 kpc, or $(m - M)_{625} = 12.33$.

Subject headings: binaries: general – globular clusters: individual (NGC 6397) – stars: imaging – stars: Population II – stellar dynamics – white dwarfs

1. INTRODUCTION

Hubble Space Telescope (HST) has opened a new era in the study of white dwarfs by making it possible to study these stars within globular clusters for the first time. Early HST observations revealed handfuls of white dwarfs in several clusters; since then, extensive cooling sequences comprising hundreds of white dwarfs have been observed in nearby clusters—e.g., Renzini et al. (1996); Cool, Piotto, & King (1996); Richer et al. (1997); Zoccali et al. (2001); Hansen et al. (2004, 2007); Calamida et al. (2008). The advantages of studying a population of stars all at the same, well-known distance can thus be brought to bear on the study of the final stage of evolution of low-mass stars.

As the second-nearest globular cluster to the Sun, and one with a well-constrained reddening (Gratton et al. 2003), NGC 6397 is particularly favorable for the study

of white dwarfs (WDs). Early HST Wide Field Planetary Camera 2 (WFPC2) observations revealed a narrow sequence of stars whose position was consistent with carbon-oxygen WDs (CO WDs) of a single mass in the range $\sim 0.5-0.6M_{\odot}$ (Cool, Piotto, & King 1996). Most recently, Hansen et al. (2007) have measured the distance and age of the cluster by detecting the bottom of the WD sequence, and Davis et al. (2008) have found evidence for natal kicks among CO WDs in the cluster. Both studies make use of deep HST/ACS imaging of a field outside the half-mass radius (Richer et al. 2008).

NGC 6397 is also the nearest apparently core-collapsed globular cluster (Trager, King & Djorgovski 1995). It has a small, resolved core of uncertain radius ($1.5 - 8''$ at 95% confidence—Sosin (1997)) surrounded by a power-law “cusp” region extending out to $\sim 100''$ (Lauzeral et al. 1992; Lugger et al. 1995). A wide variety of objects whose origins are thought to be linked to its high central density and resulting high rate of stellar interactions have been discovered in this central cusp region. These include numerous blue stragglers (Aurière, Lauzeral, & Ortolani 1990), cataclysmic variables (CVs) (Cool et al. 1995; Grindlay et al. 2001; Cohn et al. 2009), a quiescent low-mass X-ray binary (Grindlay et al. 2001), and a millisecond pulsar (MSP) (D’Amico et al. 2001).

A recent addition to the growing list of stellar exotica in NGC 6397 is a set of faint blue stars thought to be low-mass white dwarfs with helium cores (He WDs). The

¹ Department of Astronomy and Astrophysics, University of California, Santa Cruz, 287 Interdisciplinary Sciences Building (ISB), Santa Cruz, CA 95064; rstrickl@ucsc.edu

² Department of Physics and Astronomy, San Francisco State University, 1600 Holloway Avenue, San Francisco, CA 94132; cool@sfsu.edu

³ Space Telescope Science Institute, Baltimore, MD 21218; jayander@stsci.edu

⁴ Department of Astronomy, Indiana University, Swain West, Bloomington, IN 47405; cohn@astro.indiana.edu, lugger@astro.indiana.edu

⁵ Max-Planck-Institut für Astrophysik, Karl-Schwarzschild-Str. 1, Garching, 85471, Germany; aldos@mpa-garching.mpg.de

first three of these were found serendipitously in a search for CVs using HST/WFPC2 (Cool et al. 1998). Dubbed “non-flickerers,” they showed neither the short-term variability nor the UV excess typical of CVs. Three more candidates were found in a subsequent WFPC2 study that included $H\alpha$ imaging; all six candidates were found to be $H\alpha$ -faint, consistent with their proposed classification as He WDs (Taylor et al. 2001). The one candidate for which a spectrum has been obtained (NF2) revealed a broad $H\beta$ line that confirmed its identity as a low-mass white dwarf (Edmonds et al. 1999).

Helium-core WDs have the potential to provide new insight into a cluster’s population of binary stars—stars that play a critical role in globular cluster dynamics (Hut et al. 1992). The six He WD candidates identified in NGC 6397 as of 2001 are confined to the central $\sim 30''$ of the cluster, a distribution that strongly suggests the presence of unseen binary companions (Cool et al. 1998; Taylor et al. 2001). The spectrum of NF2, with its apparently Doppler-shifted $H\beta$ line, also hints at the influence of a dark, compact companion (Edmonds et al. 1999). Double-degenerate He WD binaries are of additional interest as potential progenitors of AM CVn stars (Nelemans et al. 2001b) and sources of gravitational radiation (Benacquista 2006).

In the field, He WDs are commonly found in binary systems, typically in ultra-compact X-ray binaries (ULXBs; Nelemans, Jonker, & Steeghs (2006) and references therein), as companions to MSPs (van Kerkwijk et al. 2005) or in double-WD systems (Marsh, Dhillon, & Duck 1995; Maxted, Marsh, & Moran 2002). In globular clusters, eight He WDs have been identified other than those in NGC 6397. Three are in ultra-compact X-ray binaries—in NGC 6712 (Anderson et al. 1993), NGC 6624 (Anderson et al. 1993) and M15 (Dieball et al. 2005). Three are companions to MSPs—in 47 Tuc (Edmonds et al. 2001), NGC 6752 (Ferraro et al. 2003) and M4 (Sigurdsson et al. 2003). In M4 a second He WD has been found as the companion to a subdwarf B star (O’Toole et al. 2006), while in 47 Tuc a second was identified recently in a spectroscopic study of blue stars (Knigge et al. 2008).

From an evolutionary point of view, the connection to binarity follows from the need to prevent helium ignition at the tip of the red giant branch (RGB)—otherwise a CO WD will result, as for single stars. If a giant’s envelope is removed before helium ignition, then the degenerate core will be exposed and produce a low-mass white dwarf with a helium core. Removal of the envelope may be accomplished either via Roche-lobe overflow onto a pre-existing close binary companion (Webbink 1975) or a collision between an RGB star and a compact object, leading to a common envelope phase followed by envelope ejection (Davies, Benz, & Hills 1991). Either way, the He WD is left in a binary. He WDs can also form from single stars if they can somehow lose an unusually large amount of mass while on the RGB (Castellani & Castellani 1993). However, as we will show, the radial distribution of the He WDs in NGC 6397 strongly suggests that they have binary companions, making such scenarios unlikely to apply in this case.

Here we use the Advanced Camera for Surveys’ Wide Field Channel (ACS/WFC) to study the central regions

of NGC 6397 in more detail. Our primary focus in the present paper is on the He WDs. With the wider field of view, improved spatial resolution, and greater sensitivity of ACS/WFC relative to WFPC2, we probe a larger region of the cluster to fainter magnitudes, and uncover a much larger population of He WDs than was previously known. Future papers will provide a complete analysis of the full data set and report on our search for optical counterparts of Chandra X-ray sources in these data (Cohn et al. 2009, in preparation).

Our use of the $H\alpha$ and R_{625} filters also enables us to test for the presence or absence of an $H\alpha$ absorption line in the atmospheres of the CO WDs in the WFC field and thus to classify them as either of the DA (hydrogen atmosphere) or non-DA type. The relative numbers of DA vs. non-DA WDs in globular clusters is of significant interest in view of recent findings that the incidence of non-DA stars appears to be much lower in open clusters than in the field (Kalirai et al. 2005), and outstanding questions about the mechanisms that give rise to these differences (Moehler & Bono (2008) and references therein). The possibility that the deficit of non-DA stars in open clusters may be explained as a result of the larger masses of open-cluster WDs (Kalirai et al. 2005) can be tested by observing globular-cluster WDs, whose masses are similar to those of field WDs. All WDs for which classifications have been made in globular clusters have been found to be DAs (Moehler et al. 2000, 2004). However the number classified to date is small (4-5 in each of two clusters) owing to the difficulty of spectroscopic observations of such faint stars in crowded fields.

Finally, we determine a distance to NGC 6397 using ~ 300 of the best-measured CO WDs, together with a CO WD model cooling track kindly provided by and transformed to the HST/ACS filter system by P. Bergeron (Bergeron, Wesemael, & Beauchamp 1995).

We describe the data set, together with the photometric analysis and calibration method, in §2. In §3 we identify He WD candidates using color-magnitude diagrams (CMDs). We then consider other possible explanations for stars appearing in the parts of the CMDs occupied by the He WD candidates. In §4 we compare the CO WDs to theoretical cooling tracks in a $H\alpha - R_{625}$ vs. R_{625} CMD to distinguish DA from non-DA WDs, and discuss the significance of our finding that most, and perhaps all, of the CO WDs are of the DA class. In §5 we present our distance determination. In §6, we analyze the spatial, mass, and age distributions of the He WDs, and use the results to glean information about the nature of their binary companions, the orbital periods of their progenitor binaries, and the binary fraction in the cluster. We also compare our results to predictions made by Hansen, Kalogera, & Rasio (2003) regarding the He WDs in NGC 6397. We summarize our results in §7.

2. OBSERVATIONS AND PHOTOMETRIC ANALYSIS

We obtained images using the ACS/WFC comprising a total of five short and five long exposures each in the F435W and F625W filters (hereafter $_$ and R_{625}) and 40 long exposures in the F658N filter (hereafter $H\alpha$). Ten single-orbit visits were made over the course of a year beginning 2004 July 16. During each visit, one short and one long exposure were taken in either $_$ (13 s and

340 s) or R_{625} (10 s and 340 s), followed by four 390 s or 395 s exposures in $H\alpha$. Due to the changing roll angle of the telescope over the course of the year, a mosaic constructed from all of the images in a given filter results in the pinwheel shape seen in Figure 1. The mosaic provides complete coverage out to a radius of $\sim 1'.5$ from the cluster center, partial coverage in two or more exposures out to $\sim 2'.5$, and partial coverage in at least one exposure out to $\sim 2'.9$. For comparison, the half-mass radius of NGC 6397 is $2'.33$ (Harris 1996).

Photometry was carried out using the techniques developed by J. Anderson that use an “effective” point-spread function (PSF) approach to model how the PSF varies with position on the ACS/WFC detector. These methods are described by Anderson & King (2000) and applied to the WFC by Anderson & King (2006). We constructed effective PSFs for each of the three filters from the present data set using a subset of bright, well-measured stars in each filter.

To generate a star list that would be close to complete while also excluding most artifacts, we began by finding peaks in each individual FLT-format image. We then transformed all coordinates to a common reference frame and looked for matches within 0.5 pixels. In $H\alpha$ and R_{625} , objects that created significant peaks in at least three of the five images were considered potential stars. In $H\alpha$ a larger number of matches was required, depending on the number of images in which the star could potentially have appeared (up to 40). Multiple passes of star-finding were made; during each pass, the stars found in the previous pass were removed, and additional stars were searched for in the subtracted images. When finding fainter stars, we used the method described by Anderson et al. (2008) to avoid false detections due to the ‘knotty’ PSFs and diffraction spikes associated with bright stars. The final collated list contained 25,004 stars.

For stars with $R_{625} < 18.5$, we measured magnitudes in each individual frame and then averaged together the results. This worked well for bright stars which make strong peaks in all images in which they appear. For stars bright enough to saturate in all the long exposures we adopted magnitudes derived from averages of the short exposures instead. So as to obtain a complete census of bright stars, magnitudes were measured even for stars that are saturated in the short exposures. Saturation in the short exposures reduces the accuracy of the magnitudes measured for stars with $R_{625} \lesssim 14$ (see Fig. 2).

For stars with $R_{625} > 18.5$, we combined the information from all available frames to measure a single magnitude for a given star. This produced noticeably better results for faint stars that do not necessarily produce strong peaks in every frame. By incorporating information from frames in which a given star would otherwise not have been measured, this method eliminates the bias toward brighter magnitudes that would otherwise occur for faint stars.

To calibrate the photometry we first selected one long-exposure FLT image in each filter and performed pixel area map corrections. Next we used DAOPHOT (Stetson 1987, 1994) to measure magnitudes in $0'.5$ -radius apertures for 15-20 bright, unsaturated, relatively isolated stars in each filter. We converted the resulting aperture magnitudes to the VEGAMAG system using the pre-

scriptions provided by Sirianni et al. (2005). We then found the offsets between these calibrated magnitudes and our instrumental magnitudes for the same stars. Applying these offsets to all the instrumental magnitudes then yielded calibrated magnitudes for the entire data set on the VEGAMAG system.

3. AN EXTENDED SEQUENCE OF HELIUM-CORE WHITE DWARFS

In Figure 2, we show R_{625} vs. $B_{435} - R_{625}$ and R_{625} vs. $H\alpha - R_{625}$ color-magnitude diagrams (CMDs) for the central regions of NGC 6397. Here we plot only stars that were detected in at least two frames in each filter; 15,842 stars made this cut. We further required that, in each filter, a star’s profile be reasonably well matched to the PSF at its location using the “ q ” quality-of-fit parameter described by Anderson et al. (2008)—see Strickler (2008) for details. This eliminated another 866 objects, leaving a final list of 14,976 stars that appear in these CMDs. These are the stars that we analyze in the remainder of this paper. For stars brighter than $R_{625} = 18.5$ we plot averages of magnitudes measured in individual frames. For all fainter stars we plot magnitudes derived from simultaneous fitting.

The most prominent features in these CMDs are the main sequence (MS) and the RGB, both of which appear nearly vertical in $H\alpha - R_{625}$. NGC 6397’s short blue horizontal branch, blue stragglers, and WD sequence can also be seen. In the right panel, these stars all appear to the right of the RGB or MS, consistent with the stronger $H\alpha$ absorption lines associated with hotter stars. In $B_{435} - R_{625}$ vs. R_{625} , the majority of the stars immediately to the left of the MS are likely to be from the halo/bulge background, while stars to the right of the MS include both foreground stars and MS-MS binaries (cf. Cool & Bolton (2002)).

Taking a closer look at the WDs in the left panel, we see that they form a densely populated sequence running from $R_{625} \sim 22$, $B_{435} - R_{625} \sim 0$ down to $R_{625} \gtrsim 26$, $B_{435} - R_{625} \gtrsim 1$. These are the carbon-oxygen (CO) WDs associated with single-star evolution in the cluster—stars that have turned off the main sequence within the past ~ 2 Gyr (cf. Cool, Piotto, & King (1996), Hansen et al. (2007)). In addition, one can see a group of objects that, for a given $B_{435} - R_{625}$ color, lie ~ 1 -2 magnitudes above the CO WD sequence. These stars are well separated in color from the halo stars, most of which have $B_{435} - R_{625} > 1$, and include the 6 stars previously identified as probable He WDs (see Fig. 3; Cool et al. (1998), Edmonds et al. (1999), Taylor et al. (2001)). Many more stars can now be seen in this region of the diagram. These stars are the primary focus of the remainder of this paper.

To distinguish potential He WDs from probable CO WDs we used the following procedure. We note at the outset that we do not expect to achieve a perfect separation between the two populations. Our goal is to select a set of the best He WD candidates to study in detail while also retaining for consideration marginal candidates that are less readily distinguished from the CO WDs. To this end we began by interpolating a $0.53M_{\odot}$ CO WD cooling track from the Bergeron et al. (1995) models and fitting it to a subset of the WDs chosen to be very likely CO WDs. Details of the fitting

procedure are presented in §5. A best fit was obtained for a distance of 2.34 kpc; the resulting placement of the theoretical cooling curve is shown in the close-up of the WD region (Fig. 3).

Next we selected all stars within ± 0.8 magnitudes in $B_{435} - R_{625}$ color of the theoretical CO WD cooling track, a region which should enclose all possible WDs while excluding halo stars. For each star in this region we determined the offset between its $B_{435} - R_{625}$ color and the $B_{435} - R_{625}$ color of the $0.53M_{\odot}$ cooling track at the same R_{625} magnitude. We then divided the stars into six bins: one bin for stars from $R_{625} = 18.9 - 23.5$ and five bins 0.5 magnitudes wide from $R_{625} = 23.5$ to 26.0. This division produced bins with ~ 70 -100 stars each. Next we computed the standard deviation of the color offsets within each bin. To minimize the impact of outliers (e.g., He WDs) on our determination of σ (which we wished to represent σ for the CO WDs exclusively), we iterated 2-5 times (until convergence), eliminating stars with color offsets greater than 2.5σ at the end of each iteration. For a Gaussian distribution of CO WD colors, this choice would eliminate ~ 1 CO WD in each bin. Finally, we defined a preliminary list of the best He WD candidates to be stars that landed more than 3σ away from the cooling track on the red side.

Two additional criteria were imposed before a star was put on the list of best He WD candidates. First, we required that it be brighter than $R_{625} = 24.5$, since measurement uncertainties increase rapidly for magnitudes fainter than this; the possibility that additional He WDs may lie at fainter magnitudes is considered in detail below. Second, we required that it be at least 0.75 mag brighter than the $0.53M_{\odot}$ cooling sequence to eliminate possible double CO-WDs; this last requirement eliminated two additional stars. The 24 stars that met all these criteria are marked with large open circles in Fig. 3. The six previously identified candidates (Cool et al. 1998; Taylor et al. 2001) are among these and are shaded grey. These 24 He WD candidates are listed in order of increasing R_{625} magnitude in Table 1. For each star we provide, in columns 1-8, an ID number, the x and y coordinate in our R_{625} mosaic, the R.A. and Dec. in J2000 coordinates, the radial offset from the cluster center in arcseconds, the R_{625} magnitude, the $B_{435} - R_{625}$ color, and the $H\alpha - R_{625}$ color.

To identify probable CO WDs, we followed the same procedure but used a more stringent requirement in doing the sigma clipping (2.25σ instead of 2.5σ), which yielded slightly smaller final values of σ for each bin. We then defined CO WDs to be the 438 stars that lie within $\pm 3\sigma$ in any bin. These stars are marked as large black dots in Fig. 3. Stars that lie between the CO WDs and the best He WD candidates or that failed to meet the two additional criteria described above were retained as marginal He WD candidates. These 17 stars are marked with small open circles in Fig. 3 and listed in the lower portion of Table 1.

Having defined regions in the CMD occupied primarily by CO WDs vs. He WD candidates, we wish to assess the extent to which poorly measured CO WDs might be included among either the best 24 He WD candidates or the 17 marginal ones. First we note that a close examination of the $B_{435} - R_{625}$ vs. R_{625} CMD (Fig. 3, left panel) reveals 6 stars in the range $R_{625} = 22 - 24$ that

are offset to the left of the CO WD sequence by about the same amount that the marginal candidates are offset to the right of the sequence. Thus it seems likely that the marginal group of 17 stars includes a few poorly measured CO WDs. By contrast, the best 24 candidates have no such counterparts to the left of the sequence and are likely to be a much cleaner set.

To more thoroughly assess the level of contamination among the He WDs we used artificial star tests in a manner similar to that described by Anderson et al. (2008). We added artificial stars into the individual images, and then reanalyzed the images using procedures identical to those used to analyze the data originally (see §2). A total of $\sim 100,000$ artificial stars were introduced with magnitudes in the range $R_{625} = 20 - 28$ and colors matching the $0.53M_{\odot}$ cooling sequence shown in the left panel of Fig. 3. We then used the artificial star results to construct 1000 simulated CO WD sequences by picking stars at random from the artificial stars that were recovered. For each simulated WD sequence, we extracted a number of stars equal to the number of observed CO WDs and with the same luminosity function, i.e., the same number of stars per 0.5 mag bin. In each realization, we counted how many of the artificial CO WDs had landed in the regions of the CMD previously defined to contain the 24 best and 17 marginal He WD candidates, respectively.

Among the 24 best candidates, we find that nearly all of the 18 stars with $R_{625} < 23.5$ are likely to be genuine He WD candidates: the average number of CO WD interlopers in this region in the simulated CMDs was only 0.8 ± 0.8 . Of the 6 stars with $R_{625} = 23.5 - 24.5$, about half may be interlopers, judging from the simulated CMDs. Thus roughly 20 of the 24 best candidates cannot be explained as poorly measured stars; this accords with the results of a visual inspection which revealed no sign that these stars were unusually crowded in the images. Among the 17 marginal candidates, the simulated CMDs suggest that roughly half are likely to be poorly measured CO WDs. We counted 2.8 ± 1.7 interlopers among those with $R_{625} < 23.5$ (vs. 9 observed) and 1.6 ± 1.2 interlopers in the range $R_{625} = 23.5 - 24.0$ (vs. 4 observed). For $R_{625} > 24.5$, however, the artificial CMDs produced interlopers in numbers comparable to the number of observed candidates. We conclude that few if any of the 4 faintest marginal candidates are likely to be genuine He WD candidates.

For the remainder of the paper we will focus primarily on the subset of the 24 best He WD candidates, the vast majority of which are well-measured stars, while keeping in mind that perhaps half of the brighter marginal candidates could also be genuine He WD candidates. Before going on to analyze their properties, however, we consider other possible explanations for the presence of stars in the region of the CMD that they occupy. We note that there is little question that they are cluster members: a uniform spatial distribution, as would be expected for a group of foreground or background objects, is definitively ruled out by their strong degree of concentration toward the cluster center (see §6.1). Our preliminary look at the proper motions of these stars provides independent confirmation that nearly all are cluster members; a full analysis of the proper motions is, however, beyond the scope of the present paper.

We first consider the possibility that they may be cat-

aclysmic variables (CVs), eleven of which are now known in NGC 6397 (see triangles in Fig. 3). Given that two of these CVs land in the region in the $B_{435} - R_{625}$ CMD occupied by the He WD candidates, it is natural to ask whether some of the He WD candidates could instead be CVs; this possibility was suggested by Townsley & Bildsten (2002) as a possible explanation for the three candidates identified by Taylor et al. (2001). One argument against this possibility is that while all the known CVs were found as counterparts to X-ray sources in Chandra imaging (Grindlay et al. 2001; Cohn et al. 2009), none of the 41 He WD candidates identified here have X-ray counterparts down to the limit reached with existing Chandra imaging ($L_x \lesssim 3 \times 10^{29} \text{ erg s}^{-1}$) (Cohn et al. 2009). Very few if any CVs in the field have luminosities below this limit (Verbunt et al. (1997), Pretorius et al. (2007), and references therein).

A second argument against the He WD candidates being CVs comes from comparing the locations of known CVs with the He WD candidates in the $H\alpha - R_{625}$ vs. R_{625} diagram (Fig. 3, right panel). Nine of the 11 CVs have $H\alpha - R_{625}$ colors significantly to the left of the main sequence. This implies excess emission through the $H\alpha$ filter, and in turn the likely presence of an $H\alpha$ emission line (see Grindlay et al. (1995) and Edmonds et al. (1999) for the efficacy of this method in picking out emission-line stars). Even the two CVs that lie to the right of the MS in $H\alpha - R_{625}$ are still significantly $H\alpha$ -bright compared to the WDs; comparison to the white dwarf sequence is appropriate for most of the fainter CVs, since their blue $B_{435} - R_{625}$ colors imply that their broad-band spectra are dominated by the hot WD. Thus all eleven of the CVs show strong evidence of having $H\alpha$ emission lines, which is a key signature of accretion and nearly ubiquitous in CVs (e.g., Williams (1983)). By contrast, nearly all of the He WD candidates have $H\alpha - R_{625}$ colors consistent with strong $H\alpha$ absorption lines, and very similar to those of the CO WDs in the cluster. Only one (ID=14) has an $H\alpha - R_{625}$ color close to any of the known CVs.

A second possibility to consider is that the He WD candidates could instead be detached WD-MS binaries. Like CVs, such binaries would naturally occupy the region between the MS and WD sequence (Lopez & Cool 2007). To explain the proximity of the candidates to the CO WD sequence in the $B_{435} - R_{625}$ vs. R_{625} CMD, however, would require that the MS companions all have extremely low masses. Combining the observed CO WD sequence with model MS stars from Dotter et al. (2008), we find that all but the brightest 4 He WD candidates could be explained as CO WD/MS-star binaries only if the MS star had $\mathcal{M} \lesssim 0.15\mathcal{M}_{\odot}$. Cool et al. (1998) set a similar limit on the possible presence of MS companions for the three original bright candidates using multi-band WFPC2 data. That the $H\alpha - R_{625}$ colors of the He WD candidates closely resemble those of the CO WDs also implies that if any of the candidates were CO WDs then the MS companions must contribute a small fraction of the total light of the system. As there is no reason to think that binaries in NGC 6397 should favor such low-mass companions—and exchange interactions certainly would not—we conclude that it is unlikely that many of

these stars are detached WD/MS binaries.

4. HYDROGEN VS. HELIUM ATMOSPHERES

Use of the $H\alpha$ filter enables us to determine whether hydrogen is present or absent in the atmospheres of both the CO and He WDs we observe. In Fig. 3 we have plotted a DB (helium atmosphere) cooling sequence (thick solid line) along with the DA (hydrogen atmosphere) cooling sequence (thick dash line). We interpolated these tracks for an assumed mass of $0.53\mathcal{M}_{\odot}$ from the Bergeron et al. (1995) CO WD models. In the right panel, the same two tracks are also shown shifted 0.07 magnitudes to the right (thin lines) for reasons that will be explained below.

The DA tracks span the entire range of observed magnitudes, while the DB tracks begin at $T_{eff} = 30,000\text{K}$ (just below the so-called DB gap—Liebert et al. (1986)). In $B_{435} - R_{625}$ (left panel), the DA vs. DB tracks separate by at most ~ 0.1 magnitude in color (near $R_{625} \sim 24$)—too small a separation to definitively distinguish DA from DB WDs using the present measurements. In $H\alpha - R_{625}$ (right panel), the tracks are separated by $\gtrsim 0.2$ magnitudes in the range $R_{625} = 22.5 - 25$ and as much as ~ 0.4 magnitudes near $R_{625} = 24$. Thus DA vs. DB WDs are more readily distinguished using this filter pair. Note that the DB tracks should be taken in this context to represent any non-DA-type WDs, i.e., any WD with no $H\alpha$ line, rather than DBs exclusively. We also note that the location of the DB track to the right of the main sequence in the right panel of Fig. 3 is the result of these stars being significantly hotter than the stars on the lower main sequence. Because the $H\alpha$ filter is centered at $\lambda \simeq 6584 \text{ \AA}$ (i.e., at a longer wavelength than the R_{625} filter which is centered at $\lambda \simeq 6310 \text{ \AA}$), hotter stars will naturally produce lower ratios of $H\alpha$ to R_{625} flux and correspondingly larger values of $H\alpha - R_{625}$ even in the absence of any lines.

To determine which of the WDs in NGC 6397 are likely to be DA vs. non-DA WDs, we focused initially on the CO WDs (large solid dots in Fig. 3) and proceeded as follows. First we considered only stars brighter than $R_{625} = 24.5$; for these stars, the separation between the tracks in the $H\alpha - R_{625}$ vs. R_{625} diagram is large enough relative to the spread in the measured colors of the CO WDs that we can distinguish DA from non-DA WDs (Fig. 3, right panel). An inspection of this diagram reveals that nearly all of the CO WDs follow the DA cooling track, while there is no sign of any concentration of CO WDs around the DB track. This strongly suggests that the vast majority of CO WDs in NGC 6397 are of the DA type.

We note that while the shape of the observed CO WD sequence in the $H\alpha - R_{625}$ vs. R_{625} CMD is very similar to the shape of the theoretical CO WD track (thick dashed line), there is an offset between the color of the track and the mean color of the CO WDs. We estimate that the offset is ~ 0.07 magnitudes, and surmise that it may be the result of calibration uncertainties; shifted DB and DA tracks are shown as thin solid and dashed lines, respectively. The existence of this small offset does not affect our conclusions below regarding the relative abundance of DA vs. non-DA WDs in the cluster. Nor does it affect our measurement of the distance to the cluster (see §5) which relies only on the $B_{435} - R_{625}$ vs. R_{625}

diagram.

We can make a quantitative comparison between WDs in NGC 6397 and those in the field by focusing on a portion of the CMD for which the DA to non-DA ratio in the field is known. Tremblay & Bergeron (2008) find that in the range $T_{eff} = 10,000 - 14,000K$ the ratio of DA to non-DA WDs is about 4:1. For the models we are using (and at the distance we find—see §5), this temperature range corresponds to a magnitude range of $R_{625} \simeq 23.5 - 24.5$. In this magnitude range we observe 126 CO WDs, all but one of which lies closer to the DA track than to the DB track; this number increases to four if we compare instead to the shifted tracks. If the DA/non-DA ratio matched that in the field we should have seen ~ 25 non-DA WDs. The probability of finding 4 when 25 are expected is 2.3×10^{-7} . Thus it is clear that the ratio of DA to non-DA WDs is considerably higher in NGC 6397 than in the field. Given the likelihood of a few poor measurements among the 126 CO WDs in the interval in question, it is possible that all the observed CO WDs in NGC 6397 have hydrogen atmospheres.

This conclusion does not depend on our assumption that the CO WD mass is $0.53M_{\odot}$, as the position of the tracks in the $H\alpha - R_{625}$ vs. R_{625} diagram depends only very weakly on mass. For example, the $0.51M_{\odot}$ cooling track lies much less than 0.01 magnitudes to the right of the $0.53M_{\odot}$ track in $H\alpha - R_{625}$. Because the tracks are nearly vertical in $H\alpha - R_{625}$ vs. R_{625} , our conclusion is also largely independent of the adopted distance. Changing the distance modulus by up to 0.2 magnitudes would change the $H\alpha - R_{625}$ colors of the tracks by less than 0.01 magnitudes.

These results demonstrate that the incidence of non-DA WDs is much lower in at least one globular cluster than in the field. That more than 96% of the 126 CO WDs we observe in NGC 6397 appear to have hydrogen atmospheres confirms and extends the findings of Moehler et al. (2004). Kalirai et al. (2005) found a similar preponderance of DA WDs in open clusters, and suggested that it could be the result of the higher masses of CO WDs in open clusters vs. the field. That the same phenomenon has now been seen to occur in a globular cluster, whose CO WDs have masses quite comparable to those in the field, makes it unlikely that mass could be the primary factor in determining the relative numbers of DA vs. non-DA stars.

Our findings also illustrate the power of $H\alpha$ imaging for efficiently classifying large numbers of WDs. This is particularly valuable in globular clusters in which WDs are faint and crowded by much brighter stars, making spectroscopic observations very challenging. In a single study we have increased the number of WD classifications in globular clusters by more than an order of magnitude. $H\alpha$ imaging has been validated in its ability to pick out emission-line stars (e.g., CVs) through follow-up spectroscopic observations (Grindlay et al. 1995). Further testing of the method, in the context of absorption-line stars, would be valuable to gain greater confidence that it reliably distinguishes DA from non-DA WDs.

Finally, we note that the He WDs also follow the DA cooling track (see Fig. 3, right panel), showing that they too have hydrogen atmospheres. Independent of any comparison to theoretical tracks, their distribution is well-matched to those of the CO WDs in $H\alpha - R_{625}$, and

like them shows no tendency to follow the DB track. The only apparent difference is that the spread in $H\alpha - R_{625}$ colors for the He WD candidates seems to be somewhat larger than that for the CO WDs. This could be due in part to their larger range in temperatures and masses at a given R_{625} magnitude relative to CO WDs. We have explored the effect of these parameters, however, and find that they are unlikely to be able to fully explain the apparently larger spread; it is unclear at present what the cause might be, if in fact it is significant.

5. THE DISTANCE TO NGC 6397

The distance to NGC 6397 has been subject to considerable uncertainty, with reported values ranging from 2.2 kpc (Anthony-Twarog, Twarog & Suntzeff 1992) to 2.8 kpc (Reid 1998). Most recently, Hansen et al. (2007) have detected the bottom of the CO WD sequence in an off-center field in NGC 6397 and used it to determine a distance of 2.54 ± 0.07 kpc (converting from the quoted distance modulus) and an age of 11.47 ± 0.47 Gyr. Here we use the Bergeron et al. (1995) theoretical WD cooling models to determine a distance by matching the models to the observed WD sequence in Fig. 3. We assume a WD mass in the range $0.53 \pm 0.02 M_{\odot}$, as suggested by Renzini et al. (1996) based on the luminosities of the termination of the asymptotic giant branch (AGB), the RGB tip, the horizontal branch, and post-AGB stars. This mass range is also in accord with spectroscopic mass measurements of CO WDs in NGC 6397 (Moehler et al. 2004), and encompasses the mass of $0.51M_{\odot}$ determined by Hansen et al. (2007) (see their Fig. 19). In view of the good match between the DA cooling sequence and the location of the CO WDs in the $H\alpha - R_{625}$ CMD (see §4), we also assume that all the CO WDs are of the DA type.

Starting with a $0.53M_{\odot}$ DA WD model in the $B_{435} - R_{625}$ diagram, we tested distances from 2.20 – 2.80 kpc at 0.01 kpc intervals and found the best fit value as follows. First we determined extinction values in both filters assuming $E(B - V) = 0.18$. For stars with colors of CO WDs in NGC 6397, and adopting the reddening law of Seaton (1979), we obtained $A_{435} = 0.75$ and $A_{625} = 0.48$; these values are very weakly dependent on spectral type. We then shifted the theoretical cooling sequence to account for the distance and for the extinction in both filters. Next we selected all stars within ± 0.8 magnitudes in $B_{435} - R_{625}$ color of the theoretical sequence and in the range $R_{625} = 18.9 - 26.0$, excluding known CVs. We then computed the offset in $B_{435} - R_{625}$ color between each of these stars and the theoretical sequence at the same R_{625} magnitude. To select stars likely to be CO WDs, we computed the standard deviation of these color offsets (using the bins described in §3), iterating several times and removing stars with $> 2\sigma$ deviations at the end of each iteration. This fairly stringent requirement was imposed in order to reliably remove non-CO WDs from consideration. The best fit distance was taken to be the distance that yielded a mean $B_{435} - R_{625}$ color offset closest to zero. The best fit was achieved for a distance of 2.34 kpc, or an apparent distance modulus of $(m - M)_{625} = 12.33$; the result is shown in both panels of Fig. 3 (long-dash lines).

The main contributions to the uncertainty in the distance come from uncertainties in the CO WD mass, the reddening, and the photometric calibration. Examining

the WD models, we find that a change of $\pm 0.02M_{\odot}$ from a CO WD mass of $0.53M_{\odot}$ corresponds to a change of ~ 0.05 in the R_{625} magnitude for the range of WD temperatures in question. This translates to a contribution to the uncertainty in the distance of ~ 0.05 kpc. The uncertainty in $E(B - V)$ is 0.02 magnitudes (Harris 1996), which translates to a uncertainties of 0.053 in A_{625} and 0.03 in $A_{435} - A_{625}$. Rerunning the model-fitting algorithm described above using $E(B - V) = 0.18 \pm 0.02$, we find that the uncertainty in the reddening results in an uncertainty in the distance of ~ 0.05 kpc. Finally, a maximum uncertainty in the photometric calibration of up to 0.1 mag would correspond to a distance uncertainty of ~ 0.11 kpc.

Combining these contributions to the uncertainty in quadrature yields a final estimate for the uncertainty in the distance of 0.13 kpc. Thus, with an assumed CO WD mass of $0.53M_{\odot}$, we find a distance of 2.34 ± 0.13 kpc. We note that our final result is in reasonable agreement with the distance determined by Hansen et al. (2007) if we adopt their value of $0.51M_{\odot}$ for the mass of all but the very faintest CO WDs (see their Fig. 19). In this case our distance increases to 2.39 ± 0.13 kpc, which is to be compared with their value of 2.54 ± 0.07 kpc.

6. DISCUSSION

The sequence of 24 helium-core WD candidates identified here quadruples the number known in NGC 6397. This is the first such extensive sequence of individually identified He WDs found in a globular cluster. Their presence illustrates the complexity of WD sequences in GCs, which has been extensively explored by Hurley & Shara (2003). A large population of He WDs has also been proposed to explain the total numbers and range of colors of WDs observed in ω Cen (Calamida et al. 2008). Our ability to identify individual He WD candidates in NGC 6397 presents a unique opportunity to study a large group of these rare stellar remnants all at the same, well-known distance. Given their connection to binary stars and/or stellar interactions, they provide a fresh window into the inner workings of a globular cluster.

6.1. Photometric vs. dynamical masses of the He WDs

We begin by examining the location of the He WD candidates in the $B_{435} - R_{625}$ vs. R_{625} CMD, comparing their magnitudes and colors to theoretical He WD models. These He WD models have been computed with the same code and input physics as described by Serenelli et al. (2002), and their synthetic spectra according to Rohrmann et al. (2002). Fig. 4 shows model sequences for masses ranging from 0.175 - $0.45M_{\odot}$ and $Z=0.0002$ progenitors, a metallicity appropriate for NGC 6397 (Harris 1996). Because magnitudes (and to a much lesser extent colors) depend somewhat on the thickness of the remnant’s hydrogen layer (and cooling age much more so—see below), we have computed two sets of models characterized by different H-layer masses. Models with “thick” envelopes (left panel) have H-layer masses ranging from $5 \times 10^{-3}M_{\odot}$ for the least massive model down to $4 \times 10^{-4}M_{\odot}$ for the $0.45M_{\odot}$ WD model. These models were obtained by assuming that binary evolution leads to stable mass transfer; computational details can be found in Serenelli et al. (2002). In this case

mass loss from the WD progenitor ends when the envelope mass becomes small enough that an extended structure cannot be supported any longer and then shrinks within the Roche-lobe. Models thus computed represent an upper limit to the possible H-layer thickness that a He-WD model of given mass can have. In these models, nuclear burning (mostly through the p-p chain) is a main source of energy along the WD cooling phase. On the other hand, “thin” envelope models (Fig. 4 right panel) were obtained by modifying the envelope structure of pre-WD models in such a way as to render hydrogen nuclear burning at the base of the envelopes negligible, while keeping the total WD mass fixed. In our models, this translates into “thin” H-layers with masses between $1 \times 10^{-4}M_{\odot}$ and $5 \times 10^{-5}M_{\odot}$. Our sets of “thick” and “thin” models represent the two extremes in terms of cooling timescales for He-WD stars. They also bracket reality in terms of mass-radius relations for these stars. Even thinner H-layers than those adopted in our models would not translate into noticeable smaller radii (fainter magnitudes).

Comparison to either set of models shows that most of the 24 He WD candidates (large circles) have magnitudes and colors consistent with masses in the range $\mathcal{M} \sim 0.2$ - $0.3M_{\odot}$. This is in good agreement with the mass of $\sim 0.25M_{\odot}$ determined for the one candidate for which a spectrum has been obtained (ID=2 in Table 1; Edmonds et al. (1999)). Comparing the two panels, we see that with thinner envelopes (right panel) the inferred masses shift to slightly lower values on average. This effect is particularly pronounced at the bright end (see also Hansen et al. (2003)), such that the brightest candidate lands outside the region spanned by the thin-envelope models in the right panel. Within the measurement uncertainties, the remaining candidates are all within the region spanned by either set of models. This includes candidates 4, 5, and 6, first identified by Taylor et al. (2001), whose $V_{555} - I_{814}$ colors measured from WFPC2 images appeared noticeably redder than $0.2M_{\odot}$ models (Serenelli et al. 2002). We speculate that the discrepancy may be the result of a bias toward redder measured colors for stars near the detection limit in the WFPC2 observations. In both panels of Fig. 3 the marginal candidates (small open circles) lie along tracks predicted for 0.35 - $0.45M_{\odot}$ He WDs.

An independent measure of the average mass of the He WD candidates as a group can be obtained by examining their radial distribution within the cluster. The dynamical relaxation time at the half-mass radius ($r_h = 2'33$) is $\sim 3 \times 10^8$ years; at the center it is less than 10^5 years (Harris 1996). As all the He WD candidates are well inside the half-mass radius (and half of the best 24 are less than $30''$ from the center), their radial distribution should reflect their masses. Indeed, a high degree of mass segregation in the central regions of NGC 6397 has been well documented (King, Sosin, & Cool 1995).

In Fig. 5 we plot the cumulative radial distribution of the 24 best He WD candidates (solid black line) along with that of several other populations in the cluster: CO WDs (short-dash line), turnoff stars (long-dash), blue stragglers (dash-dot), and the 17 marginal He WD candidates (solid grey line). We also plot the cumulative distribution that would be expected for a spatially

uniform distribution of objects (dotted line). Applying the Kolmogorov-Smirnov test to compare distributions, we find first of all that the 24 best He WDs have a $2 \times 10^{-7}\%$ chance of being drawn from a spatially uniform distribution, which definitively rules out a population of foreground or background interlopers. They are also significantly more centrally concentrated than the CO WDs (0.02% probability of being drawn from the same population) and main-sequence turnoff stars (0.2% probability). This strongly suggests that, on average, their masses are in excess of the turnoff mass of $\sim 0.8M_{\odot}$. These comparisons do not take account of incompleteness, except that we excluded CO WDs fainter than $R_{625} = 24.5$ (the magnitude of faintest of the good He WD candidates). The greater difficulty of detecting He WDs as compared to turnoff stars in the central regions would only make the difference in radial distribution more pronounced. Of all the groups to which we compare the He WDs, they most closely resemble the blue stragglers (44.1% probability), which have a range of masses $\sim 0.8-2M_{\odot}$ (Saffer et al. 2002; De Marco et al. 2005).

In contrast to the 24 best He WD candidates, the 17 marginal candidates are not nearly as concentrated to the center as the blue stragglers (K-S probability = 0.16% of being drawn from the same population; see Fig. 5). They most closely resemble the CO WDs (94.3%), though are also compatible with turnoff stars (48.8%). The probability that these 17 stars are drawn from the same population as the 24 best candidates is only 1.0%. Given the significant degree of contamination that we expect among these marginal candidates (roughly half are likely to be poorly-measured CO WDs—see §3), the similarity of their radial distribution to that of the CO WDs is perhaps not surprising. Still, if the other half really were He WDs, and these had masses comparable to those of the 24 best candidates, one might expect a greater degree of central concentration. We conclude that either the degree of contamination is greater than we estimated or that the He WDs that do exist among these marginal candidates may not have the large dynamical masses characteristic of the 24 best candidates. In view of the uncertain status of the marginal candidates, we hereafter focus our attention primarily on the 24 best candidates.

6.2. Nature of the binary companions

The mismatch between photometric masses determined from the CMD and dynamical masses determined from the radial distribution for the 24 best He WD candidates can be understood if they have binary companions of sufficient mass. Such companions are expected on evolutionary grounds (see §1) and earlier observations found evidence for them (Cool et al. 1998; Edmonds et al. 1999; Taylor et al. 2001). Here we use the measured dynamical vs. photometric masses of the He WDs to place new constraints on the nature of these companions.

Given that the bulk of the He WD candidates have photometric masses in the range $0.2-0.3M_{\odot}$, whereas the dynamical masses resemble those of the much more massive blue stragglers ($0.8-2M_{\odot}$), the companions must make up this large mass deficit. We note that the blue straggler mass range found by De Marco et al. (2005) is based on six of the brightest blue stragglers in NGC 6397

and thus may not be representative of the entire population of 24 blue stragglers in our sample. To estimate the typical blue straggler mass, we have performed cored power-law fits to the radial distributions of turnoff stars and blue stragglers (Cohn et al. 2009). Taking these two groups to be in approximate thermal equilibrium results in a blue straggler mass of $1.2 \pm 0.1M_{\odot}$. Adopting this as the typical mass for the He WD binary systems suggests a companion mass of $\sim 1M_{\odot}$. This rules out main-sequence companions, as MS stars near the turnoff mass would dominate the light and cause the He WD binaries to be significantly brighter and redder than is observed. CO WDs with masses $\sim 0.53M_{\odot}$ (like those currently being produced in the cluster) are also ruled out, since they fall well short of the required companion mass. We have also compared the observed radial distribution of the He WDs to the expected distribution of $1.6M_{\odot}$ stars (i.e., the dynamical mass of a He WD binary containing a neutron star) and find that $1.4M_{\odot}$ companions are ruled out, even when we allow for incompleteness in the He WD distribution. Thus we conclude that the required typical mass of the unseen companions of about $1M_{\odot}$ is most compatible with heavy WDs.

The non-detection in X-rays of any of the 41 He WD candidates further supports the view that the companions are white dwarfs rather than neutron stars. NSs should have been spun up to become MSPs during the mass-transfer stage. For comparison, the 19 MSPs in 47 Tuc have $L_x \sim 10^{30} - 10^{31} \text{ erg s}^{-1}$ (Bogdanov et al. 2006); if any of the He WDs in NGC 6397 had comparable MSP companions they should have been seen in existing Chandra imaging that reaches $L_x \lesssim 3 \times 10^{29} \text{ erg s}^{-1}$ (Cohn et al. 2009).

Our finding that the companions are most likely to be white dwarfs is in good agreement with the conclusions of Hansen et al. (2003), who argue on theoretical grounds that the companions to the He WDs in NGC 6397 should be WDs and not neutron stars (NSs). A key part of their argument is that mass transfer from a $\sim 0.8M_{\odot}$ turnoff star onto a NS would be stable, whereas onto a WD it would be unstable. Stable mass transfer would yield relatively wide binaries which would be vulnerable to rapid breakup in the dense environs of the center of NGC 6397. Unstable mass transfer onto a WD would instead yield tight binaries (following a period of common-envelope evolution) which would be more resilient. We note that the latter scenario would apply to mass transfer onto white dwarfs with mass less than $\sim 1M_{\odot}$, but not for more massive WDs—a point we will return to below.

6.3. Formation rate of He WDs and implications for binary population

We can use cooling ages from the He WD models to consider what the distribution of He WDs in the CMD implies about the formation rate of these stars in NGC 6397. This in turn can provide insight into the viability of different models and/or formation scenarios. The analysis is complicated by the fact that cooling ages are highly dependent upon the assumed mass of the residual hydrogen layer, with thicker layers leading to slower rates of cooling. Because thick hydrogen layers support hydrogen burning, WD evolution along the cooling sequence for thick-envelope models is completely dominated by nuclear burning on the very long

timescales dictated by the pp-cycle. By contrast, thin H envelopes render nuclear burning negligible so that for thin-envelope models, WD evolution is driven solely at the expense of the star’s internal heat. The differing rates of cooling can be seen in Fig. 4 by comparing the left and right panels, where “+” symbols are used to indicate cooling ages. In the left panel, marked ages are 1 – 13 Gyr in 1-Gyr intervals. In the right panel, they indicate ages of 0.001, 0.0025, 0.005, 0.0075, 0.01, 0.025, 0.05, 0.075, 0.1, 0.25, 0.5, 0.75, 1.0, 1.25, 1.5, 1.75, 2.0, 2.25, 2.5, and 2.75 Gyr. Thus, for example, the brightest of the three He WD candidates identified by Taylor et al. (2001) at $R_{625} \simeq 22.5$ has a cooling age of ~ 8 Gyr according to the thick-envelope models (left panel) vs. an age of only ~ 0.1 -0.25 Gyr according to the thin-envelope models (right panel). We caution that the very youngest ages shown for the thin-envelope models (on the order of 1 Myr) are uncertain by a factor of a few due to the fast initial rate of evolution and the somewhat ad-hoc nature of the models.

Here we examine the implications of thin vs. thick envelopes in turn. It should be emphasized that these models represent only two possible sets of H envelope masses. However, they represent the two opposite extremes both in terms of cooling ages and mass-radius relations and thus should bracket reality.

Considering the thin-envelope models first (Fig. 4, right panel), we see that the 24 best He WD candidates have implied cooling ages ranging from $\lesssim 1$ Myr for the brightest candidate to about 1 Gyr for the faintest. The implied formation rate is then $\sim 24 \text{ Gyr}^{-1}$. This is higher than the rate at which RGB stars and compact objects collide in the central regions of NGC 6397. Assuming then that the He WDs are instead the products of pre-existing binaries, the formation rate is determined by the fraction of stars that have a close white dwarf companion when they ascend the giant branch. The implied binary fraction can thus be determined by comparing the rate of formation of He WDs to the rate at which stars are turning off the main sequence in the same region. Counting stars above the turnoff at $R_{625} = 16.1$, we find ~ 700 subgiant and red giant stars. Considering the ~ 1.5 Gyr spent in these stages combined (Pols et al. 1998), this implies that stars are turning off the main sequence at a rate of about 470 Gyr^{-1} at the present epoch. Similar rates are implied by the number of horizontal-branch stars observed (48, which given a lifetime of ~ 0.1 Gyr implies a rate of 480 Gyr^{-1}) and by the number of CO WDs with ages of 1 Gyr or less (~ 480 after correcting for incompleteness). Thus the implied binary fraction is $24/470$ or about 5%. This is a small enough fraction that it is not surprising that the horizontal-branch and CO WD populations do not appear to be depleted by losses to He WD formation.

The $\sim 5\%$ binary fraction required to account for the observed He WDs in the context of thin-envelope models represents a lower limit on the total binary population in the central regions of the cluster, as it accounts only for the particular class of binary that yields He WDs. The $\lesssim 5$ -7% binary fraction found among MS-MS binaries in the central region of the cluster by Cool & Bolton (2002) would be in addition to the He WD progenitor binaries. The total will be less than the sum if some

MS-MS binaries are themselves progenitors of the binaries that lead to the He WDs, i.e., if a CO WD replaces one of the MS stars through an exchange collision before the other MS star turns off the main sequence (or at least before it climbs far enough up the giant branch to fill its Roche lobe). Such exchanges are not uncommon in N-body simulations of high-density clusters (e.g., Ivanova et al. (2006)).

Interpreting the He WDs in the context of thin H-envelope models implies a binary fraction that is quite plausible. However, it does present one problem. The implied cooling ages of the brightest four candidates are very young, in the range of only ~ 1 -2 Myr. It would be surprising to catch any He WDs so early in their evolution, even considering the factor of a few uncertainty in the cooling ages of such young objects. These stars cannot just be a small number of interlopers unrelated to the cluster. Three have already been shown to be proper-motion members (Cool & Bolton 2002), and our preliminary analysis shows that the fourth is as well. Such young ages would imply an implausibly high rate of formation in the very recent past, nominally on the order of 2 Myr^{-1} . Even taking the uncertainty in their ages into account, the present-day rate of formation would be more than an order of magnitude greater than the average rate over the past 1 Gyr. The current formation rate would also have to be higher than the total rate at which stars are turning off the main sequence at present ($\sim 0.5 \text{ Myr}^{-1}$). Yet only a fraction of these turnoff stars can be members of binaries that will produce He WDs. Thus it seems highly unlikely that these bright stars can be explained as He WDs with thin H envelopes.

Examining the cooling ages in the context of thick H-envelope models instead (Fig. 4, left panel), the He WDs would have ages ranging from $\lesssim 1$ Gyr to ~ 13 Gyr. In this case, the formation rate problem for the brightest candidates disappears, owing to the much slower rate of cooling associated with thick envelopes. The implied rate of formation in the recent past is $\sim 5 \text{ Gyr}^{-1}$, easily compatible with a binary formation scenario, as it would require that only $\sim 1\%$ of the stars turning off the main sequence produce He WDs in the present epoch. This rate of formation is also low enough that collisions between RGB stars and CO WDs could make a significant contribution to their production. The rate is also not too different from the long-term formation rate of $\sim 2 \text{ Gyr}^{-1}$ implied by seeing 24 He WD candidates with ages up to ~ 13 Gyr. Indeed, a moderate increase in production rate would not be surprising considering the inevitable dynamical evolution of the cluster on this timescale.

In summary, either thick or thin envelopes can explain the observations with reasonable implications for the formation rate of He WDs ($\sim 2 - 24 \text{ Gyr}^{-1}$) and the binary fraction in the cluster ($\sim 1 - 5\%$). The one exception is that the brightest candidates cannot be readily explained in the context of thin envelopes, as they would require an exceedingly high rate of formation in the very recent past.

Additional insight into the population of He WD progenitor binaries can be gleaned by examining the distribution of He WD masses, as inferred from their positions in the CMD. The mass of the degenerate core that will be left behind when a giant loses its envelope to a binary companion depends on how far up the RGB the giant

has climbed before overflowing its Roche lobe. This in turn depends on the orbital period of the binary: longer period systems, being wider, allow the giant (and the mass of its He core) to grow larger before the envelope is lost. The He WD masses we deduce from the CMDs are mostly rather small. All but 2 of the 24 best candidates have implied masses in the range $\sim 0.2 - 0.3 M_{\odot}$. This in turn implies that the progenitor binaries have periods in the range $\sim 1 - 20$ days (Rappaport et al. 1995). Longer-period binaries containing CO WDs and MS turnoff stars or giants appear to be significantly more rare, given our finding (see §3) that at most ~ 6 of the marginal candidates with $R_{625} = 22 - 24$ are likely to be genuine He WDs.

6.4. Termination of the He WD sequence

Irrespective of the thickness of H envelopes, the He WD sequence comes to a relatively abrupt end near $R_{625} \sim 24$. The dearth of He WD candidates at fainter magnitudes is readily visible in the Fig. 4 CMDs (recall from §3 that our artificial star tests show that the four faintest marginal candidates are likely to be poorly measured CO WDs). By contrast, the number of observed CO WDs is continuing to rise below $R_{625} \sim 24$. The lack of fainter He WDs cannot be the result of incomplete recovery of faint stars. Artificial star tests show that in the bins from $R_{625} = 24.5 - 25.0$ and $25.0 - 25.5$, the completeness is still $\sim 60\%$ and 50% , respectively (see Fig. 6, top panel). Thus it is unlikely that any significant number of fainter He WDs is present. When we correct for incompleteness (see Fig. 6, panels 2-4), the CO WD luminosity function continues to rise to the limit of our observations, whereas the number of He WDs is clearly in decline.

To further examine the significance of the absence of convincing He WD candidates below $R_{625} \sim 24.5$, we measured the offsets in color from the $0.53 M_{\odot}$ CO WD cooling track for each of the CO WD and He WD candidates. Fig. 7 shows color offset distributions for stars with $R_{625} = 19 - 24.5$ (left panel) and $R_{625} = 24.5 - 26$ (right panel). The distribution of the brighter stars is clearly bimodal, with the He WD candidates forming a peak centered ~ 0.4 magnitudes redward of the CO WD sequence. For the fainter stars, the color spread is larger due to growing measurement uncertainties. Still, there is no sign of any excess of stars on the right side ($\Delta(B_{435} - R_{625}) \gtrsim 0.3$) where He WDs would be expected to lie. We estimate that at most ~ 10 He WDs (2σ upper limit) could hide in the wings of the CO WD distribution in the magnitude range $R_{625} = 24.5 - 26$.

The significance of the termination of the He WD sequence is different in the context of thin vs. thick H-envelope models. If the hydrogen envelopes are thin, the sequence ends at ~ 1 Gyr, well below the age of the cluster. Such a termination was predicted by Hansen et al. (2003), who suggested that within ~ 1 Gyr, binaries containing He WDs would either merge via gravitational-wave radiation or be broken up in exchange interactions. The He WDs, as the lowest-mass stars in most such exchanges, would typically be removed from the binary and quickly redistribute themselves according to their single-star mass. While we find that the sequence extends about one magnitude fainter than predicted by Hansen et al. (2003) (who suggested that none fainter than those identified by Taylor et al. (2001) would be found in deeper

searches), our finding agrees with their prediction within the large uncertainties in cooling age associated with the unknown H-envelope thickness. In particular, while their “moderate” H envelope models put the cooling age of the faintest Taylor et al. (2001) candidate at ~ 1 Gyr, the “thin” H-envelope models we use here result in more rapid cooling, such that the He WDs are a magnitude fainter at 1 Gyr.

While our observations confirm the prediction by Hansen et al. (2003) that the sequence should end at ~ 1 Gyr, there is still a puzzle. This prediction was made specifically for the cluster core, assuming a central mass density of $1.5 \times 10^6 M_{\odot} \text{ pc}^{-3}$. Yet few, if any, of the He WD candidates are actually in the cluster core, which is very small. Sosin (1997) found a core radius of $1.5 - 8''$ at 95% confidence, while our preliminary analysis of the present data set suggests a radius in the range $\sim 5 - 7''$. Outside the cluster core, in the so-called “cusp” region, the density falls off approximately as $(r/r_c)^{-2}$. Given that a binary’s lifetime to exchange is inversely proportional to the density, a binary that would last only 1 Gyr in the core would survive more than a Hubble time at just $4r_c$. Depending on the core radius, between half and all the He WD candidates are outside $4r_c$, where the lifetime to exchange would be even longer. Thus it is not clear that the termination of the sequence can be explained in this way. N-body simulations that can more directly assess the longevity of binaries, without the simplifying assumption that they reside at a fixed radius, would be valuable.

In the context of thick envelopes, as illustrated in the left panel of Fig. 4, the faintest of the He WD candidates would have cooling ages of ~ 13 Gyr. Very old He WDs could have evolved from main-sequence stars with masses of $\gtrsim 2 M_{\odot}$, whose MS lifetimes are $\lesssim 1$ Gyr (Pols et al. 1998). Such stars have core masses $\lesssim 0.3 M_{\odot}$ as they are leaving the main sequence (Nelemans et al. 2001a). Using the present thick-envelope models, the total inferred ages would be uncomfortably high considering recent age determinations for the cluster: 12 ± 0.8 Gyr (Anthony-Twarog & Twarog 2000) and 11.47 ± 0.47 Gyr (Hansen et al. 2007). This alone should not rule out thick envelopes, however. Given the strong dependence of cooling rates on H envelope mass, even slightly lower envelope masses would likely bring the ages into agreement. Moreover, the argument against thick envelopes put forward by Hansen et al. (2003) rests in large part on their finding that binaries in the core will either merge or be broken up after 1 Gyr. They also suggest that common-envelope (CE) evolution will lead to thin H envelopes. However, in view of the location of many of the binaries outside the cluster core, and the lack of direct evidence that CE evolution leaves behind thin envelopes, we conclude that thick envelopes are not ruled out.

Another possibility is that the He WDs could be a mixture of systems, some with thick and others with thin H envelopes. If common-envelope evolution does lead to He WDs with thin envelopes (Hansen et al. 2003), then all systems for which a $\sim 0.8 M_{\odot}$ giant overflows its Roche lobe onto a CO WD companion with $M \lesssim 1 M_{\odot}$ should have thin envelopes and cool off quickly. For giants with CO WD companions of larger mass, however, the mass transfer would be stable. If thick envelopes were the re-

sult, then this subset of systems would cool much more slowly. The brightest systems in NGC 6397 could potentially be explained as such higher-mass binaries.

This hypothesis is appealing in that it could help make sense of two other ways in which the four brightest He WDs seem to set themselves apart from the remaining 20 He WD candidates. First, their apparently greater concentration toward the center (median radial offset of $12''$ vs. $33''$ for the fainter 20) could be explained as the result of mass segregation. Second, the 1.6-magnitude gap between the four brightest He WDs and the remaining systems could be the result of two very different rates of cooling. Judging from the models shown in Fig. 4, the youngest thick-envelope stars would have ages similar to the oldest thin-envelope stars (~ 1 Gyr). He WDs formed via stable mass transfer should have relatively long periods following the mass transfer episode: $\sim 2-40$ days for $0.2-0.3M_{\odot}$ He WDs (Rappaport et al. 1995). These binaries would be more vulnerable to exchange interactions than post-common-envelope binaries which would have much shorter periods. Nevertheless, at the range of radii where the four bright He WDs lie ($\sim 6-24''$), systems with 2-day periods could survive $\sim 0.6-10$ Gyr, while systems with 40-day periods could survive $\sim 0.08-2$ Gyr before the He WD would be exchanged out of the binary (cf. Hansen et al. (2003)). We surmise that the few we see concentrated to the cluster center could be the remnant of a larger population of such systems.

Finally, we note that the possibility that some He WDs could be torn away from their binary companions via exchange interactions raises the question of where these stars would be at present, and whether a second population of He WDs might be observable in the cluster. It may be that such stars would acquire high enough recoil velocities during exchange interactions that they would simply be ejected from the cluster. Escape from the cluster would follow, for example, if a $0.2M_{\odot}$ He WD in a 10-day binary with a $1M_{\odot}$ CO WD acquired a velocity comparable to its orbital velocity of $\sim 90 \text{ km s}^{-1}$. If, however, He WDs are retained in the cluster following exchange interactions, their half-mass radius should be larger than that of the cluster as a whole ($r_h \sim 140''$), due to their very low masses.

To estimate how many such isolated He WDs would still lie within the field of view spanned by the present observations, we first note that any thin-envelope He WDs older than 3 Gyr would be fainter than the detection limit (see Fig. 4, right panel). Scaling from the 24 He WDs with ages of 1 Gyr or less, we estimate that another ~ 50 would have cooling ages in the range 1–3 Gyr. Using the radial distribution of $0.25M_{\odot}$ stars in the Fokker-Planck models of NGC 6397 developed by Dull (1996), and assuming that all 50 of these He WDs have been exchanged out of binaries, we estimate that ~ 8 isolated He WDs would currently lie within a radius of $1.5'$. This is just barely compatible with our finding above that up to ~ 10 He WDs could hide in the broad wings of the CO WD distribution at very faint magnitudes in the CMD.

Using the same approach we can ask how many isolated He WDs would be present in the off-center field studied by Richer et al. (2008). Assuming that He WDs could be detected with ages up to ~ 10 Gyr in that field, we estimate that ~ 7 isolated He WDs would be present in their full ACS/WFC field. Taking a look at the CMD for

that field (see their Fig. 3), there is no clear sequence of He WDs, but there are nevertheless several stars in the region such stars would occupy. Since it is possible that these stars are unrelated to the cluster, we also inspected their proper-motion-cleaned CMD (their Fig. 5). In this CMD, only 2 stars are present in the He WD region. However, this CMD excludes roughly 40% of the area of the original field (the area not covered by the 1st-epoch WFPC2 data), such that we would predict the presence of ~ 4 isolated He WDs, consistent with what is seen. We conclude that current observations do not rule out the existence of a second population of very faint, isolated He WDs in NGC 6397.

7. SUMMARY AND CONCLUSIONS

We have identified a set of 24 faint blue, $H\alpha$ -faint stars in the globular cluster NGC 6397 that are good candidates to be white dwarfs with helium cores. This is the first extended sequence of He WDs found in a globular cluster. The masses of the He WD candidates that we infer from comparisons to the colors and magnitudes of theoretical cooling models are in the range $\sim 0.2-0.3M_{\odot}$. Dynamical masses inferred from the radial distribution are significantly higher, on the order of $1.2M_{\odot}$, implying the presence of binary companions. Constraints from the observed colors of the He WDs and their lack of X-ray counterparts suggest that the companions are most likely to be heavy white dwarfs.

The rate of formation of He WDs that can be inferred from their distribution in the color-magnitude diagram is highly dependent on their rate of cooling, which in turn depends on the uncertain thickness of their hydrogen layers. We compare the observed systems to two set of models, one with thick and the other with thin H envelopes, and infer that $\sim 1-5\%$ of stars currently turning off the main sequence eventually become He WDs. This can be understood if $\sim 1-5\%$ of main-sequence stars have or obtain CO WD companions by the time they begin evolving up the RGB. Initial binary periods of $\sim 1-10$ days are required to produce He WDs with the masses we observe. We note that this binary fraction is a lower limit to the overall binary fraction in the cluster, as it accounts only for the subset of binaries that yields He WDs with CO WD companions.

The He WD sequence ends about 1.5 magnitudes above the limiting magnitude of our study. The interpretation of this termination is different in the context of thick vs. thin H envelopes. In the case of thick envelopes, the faintest observed systems have ages comparable to the age of the cluster. In the case of thin envelopes, the faintest have ages of ~ 1 Gyr. Neither the thick nor thin envelopes considered here provide a completely satisfactory explanation for the current observations. It does seem clear that the brightest four He WDs have thick H envelopes, as thin envelopes would imply very young ages that in turn would require an implausibly high rate of He WD formation at the present epoch. If the rest have thin envelopes then the termination of the He WD sequence must be explained. The suggestion by Hansen et al. (2003) that mergers and/or exchanges destroy the binaries after ~ 1 Gyr appears viable, and could perhaps be tested by wider-area searches for faint He WDs in off-center fields. If all He WDs have thick H envelopes, then the envelope thickness must be some-

what lower than what we have assumed here in order for the oldest observed He WDs to have cooling ages compatible with the age of the cluster.

Nearly all of the CO WDs brighter than $R_{625} \sim 24.5$ ($T_{eff} > 10,000\text{K}$) have $H\alpha - R_{625}$ colors that strongly suggest that they have the broad $H\alpha$ absorption lines characteristic of DA-type (hydrogen-atmosphere) WDs. This suggests that whatever mechanism is operating to produce DBs (or other non-DA type WDs) in the field is ineffective in NGC 6397. White dwarf mass is unlikely to be the primary factor determining the relative abundance of DA vs. non-DA WDs since the masses of CO WDs in NGC 6397 are similar to those of CO WDs in the field. The 126 stars in our sample of tentatively classified CO WDs represents the largest sample of WDs for which atmospheric classifications have been obtained in a single cluster. While further validation of the method is needed to ensure that it reliably distinguishes DA from non-DA WDs, $H\alpha$ imaging should be a powerful tool to classify white dwarfs in star clusters.

Finally, we have compared the observed CO WD sequence to theoretical cooling models to measure a distance to NGC 6397. With an assumed CO WD mass of $0.53M_{\odot}$ and reddening of $E(B - V) = 0.18$, we obtain a distance of 2.34 ± 0.13 kpc.

We gratefully acknowledge Pierre Bergeron for providing CO WD models in HST/ACS filters, and for thoughtful comments; Onno Pols and Aaron Dotter for making useful RGB and MS models available online; Liliana Lopez and Jason Kalirai for helpful and interesting discussions; and the anonymous referee for providing helpful comments which improved the paper.

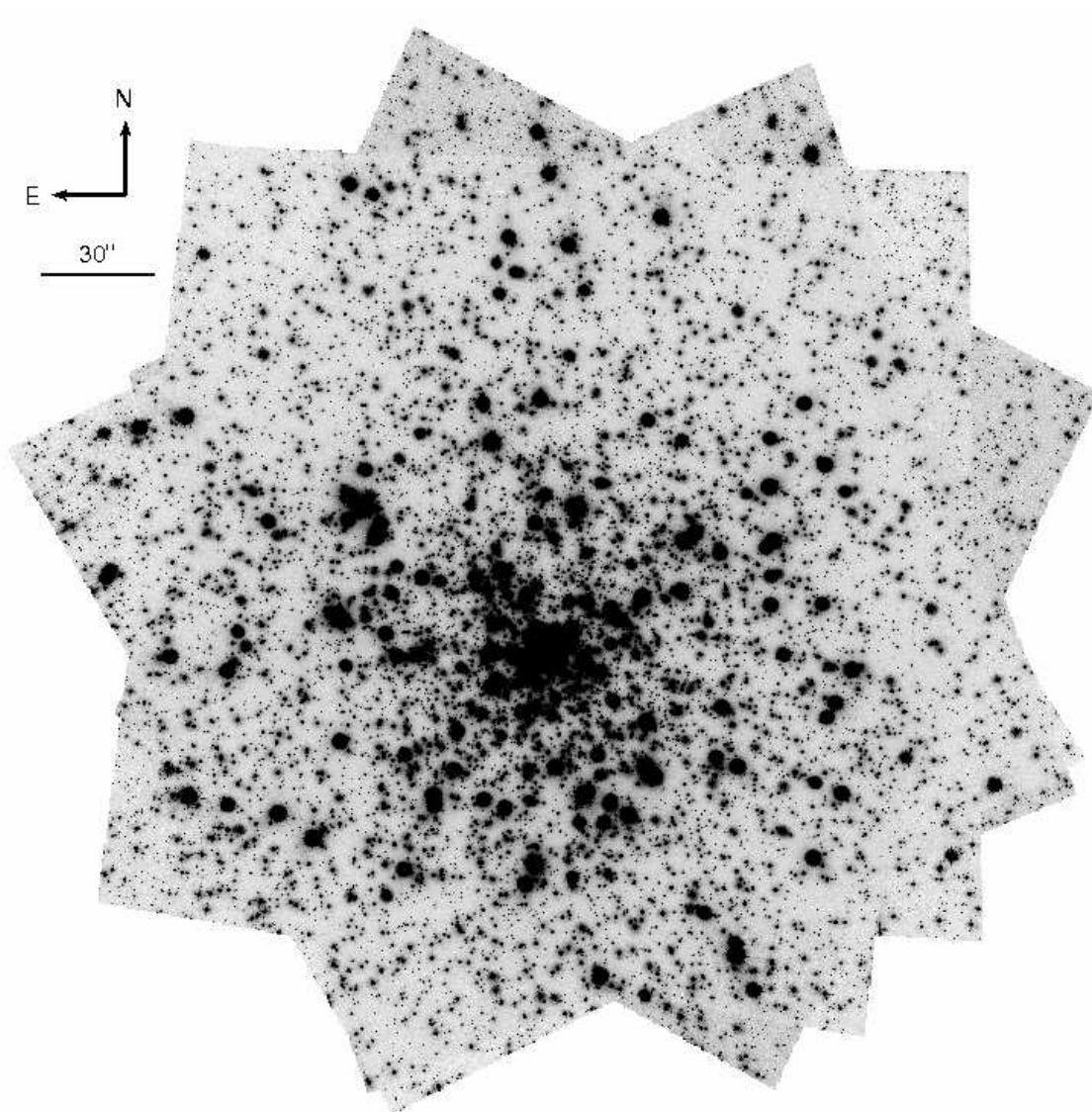


FIG. 1.— Mosaic image of NGC 6397 in the `_filter`, constructed from images taken on five visits spread over one year.

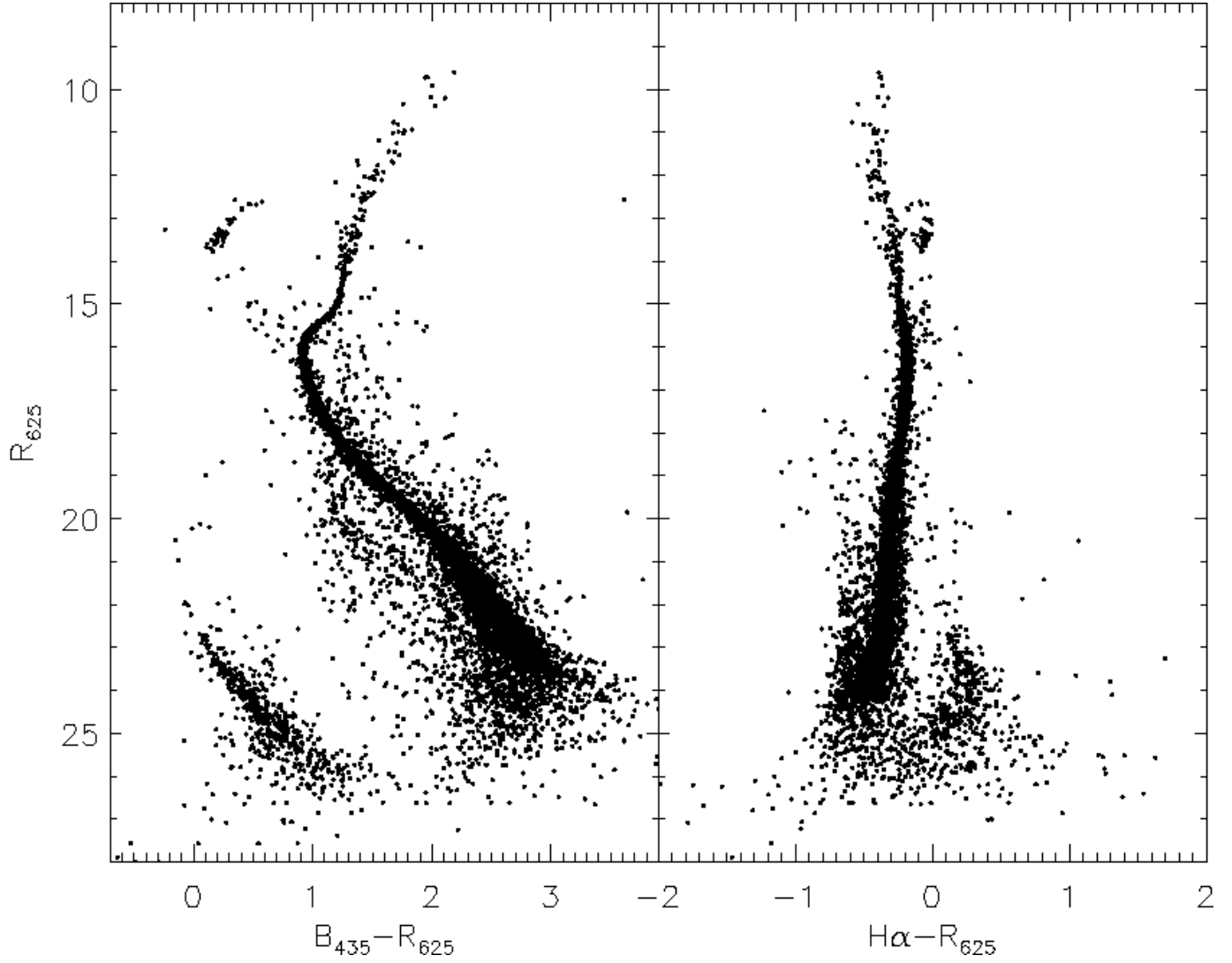


FIG. 2.— Color-magnitude diagrams for 14,976 stars in the central regions of NGC 6397. The white dwarfs on the bottom left side of the R_{625} vs. $B_{435} - R_{625}$ diagram (left panel) are the focus of this paper. In $H\alpha - R_{625}$ vs. R_{625} these stars appear to the right of the main sequence, indicating strong $H\alpha$ absorption lines.

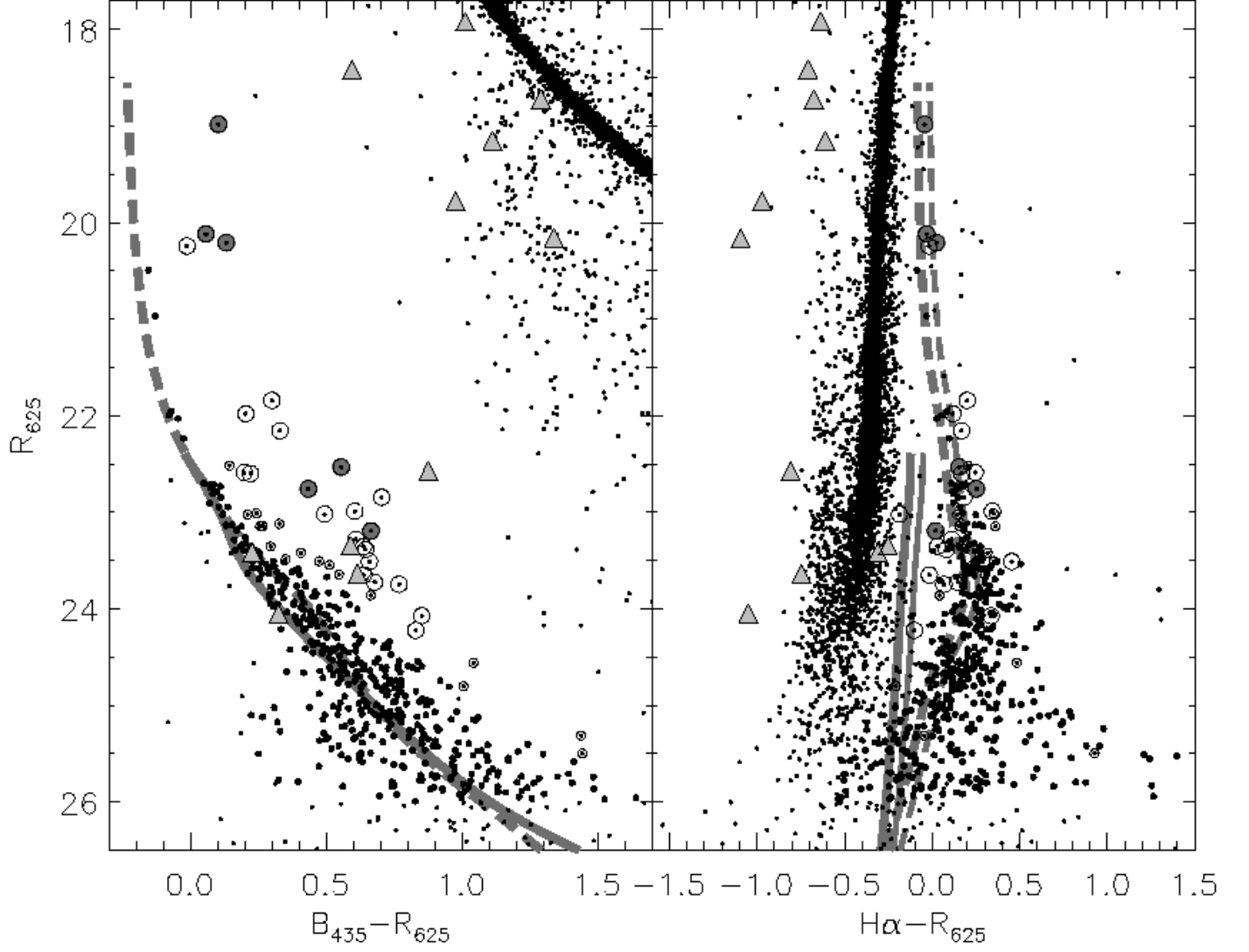


FIG. 3.— White dwarfs in NGC 6397. The 24 stars that we identify as the best He WD candidates are marked with large open circles. These include 6 previously known candidates which are shaded grey. Marginal He WD candidates (another 17 stars) are marked with small open circles. Grey triangles mark the 11 known cataclysmic variables in the cluster. Stars selected as probable CO WDs are shown as large solid dots. All other stars are shown as small dots. The thick dashed and solid lines in both panels represent $0.53M_{\odot}$ DA and DB WD cooling tracks, respectively, shown at the best-fit distance found in §5. In the $H\alpha - R_{625}$ vs. R_{625} CMD, the same pair of tracks is also shown shifted 0.07 magnitudes to the right (thin lines) to better align the DA track with the observed WDs (see §4).

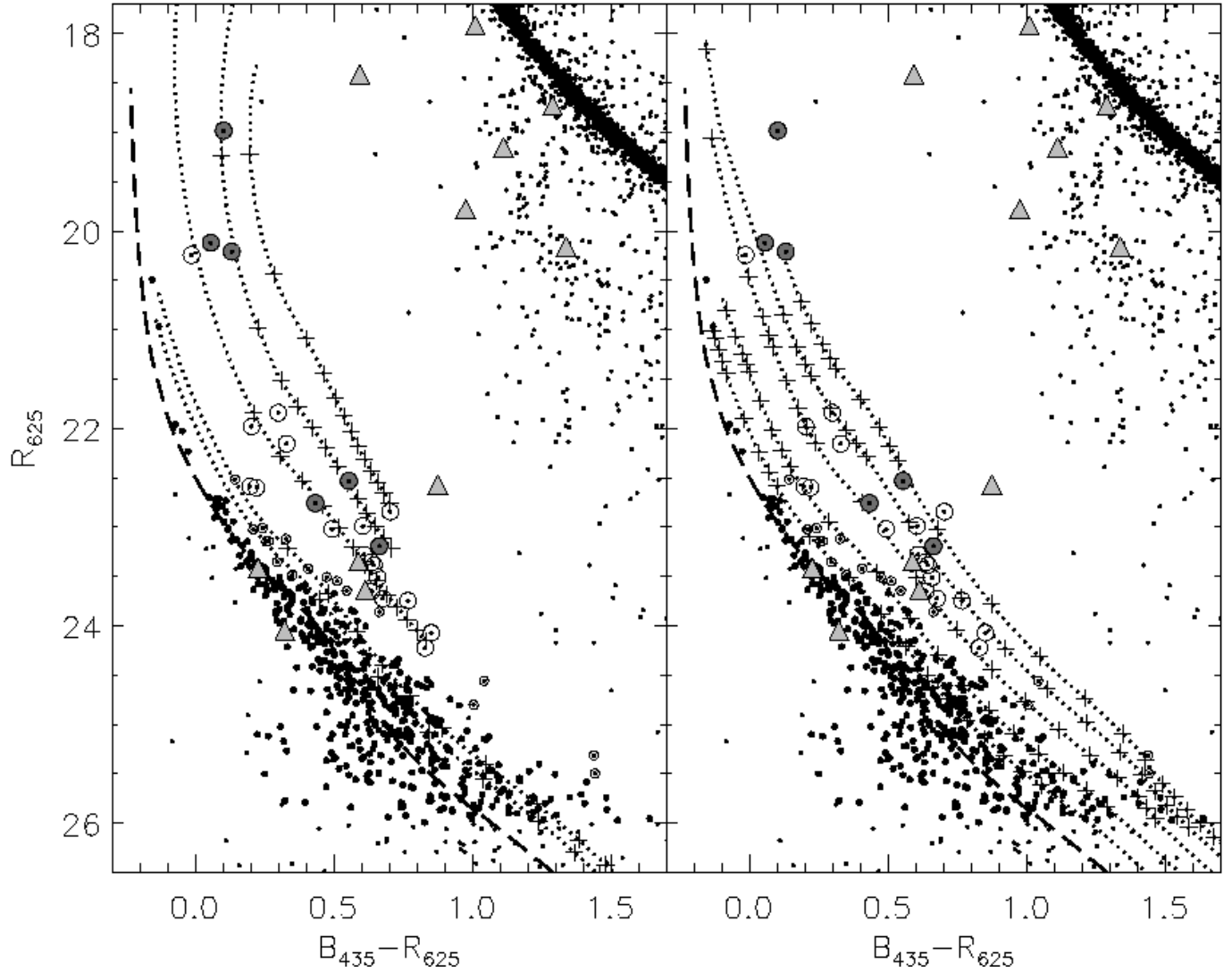


FIG. 4.— Same as Fig. 3 but with He WD cooling tracks from low-metallicity progenitors ($Z=0.0002$) overlaid (dotted lines) (Serenelli et al. 2002). The left and right panels show models with thick and thin hydrogen envelopes, respectively (see §6.1). In both panels, tracks are for He WDs with masses of $0.175M_{\odot}$, $0.20M_{\odot}$, $0.25M_{\odot}$, $0.35M_{\odot}$, and $0.45M_{\odot}$ (top to bottom). In the left panel (thick envelopes), the “+” signs indicate ages from 1 – 13 Gyr in 1 Gyr intervals. In the right panel (thin envelopes), the “+” signs indicate ages of 0.001, 0.0025, 0.005, 0.0075, 0.01, 0.025, 0.05, 0.075, 0.1, 0.25, 0.5, 0.75, 1.0, 1.25, 1.5, 1.75, 2.0, 2.25, 2.5, and 2.75 Gyr.

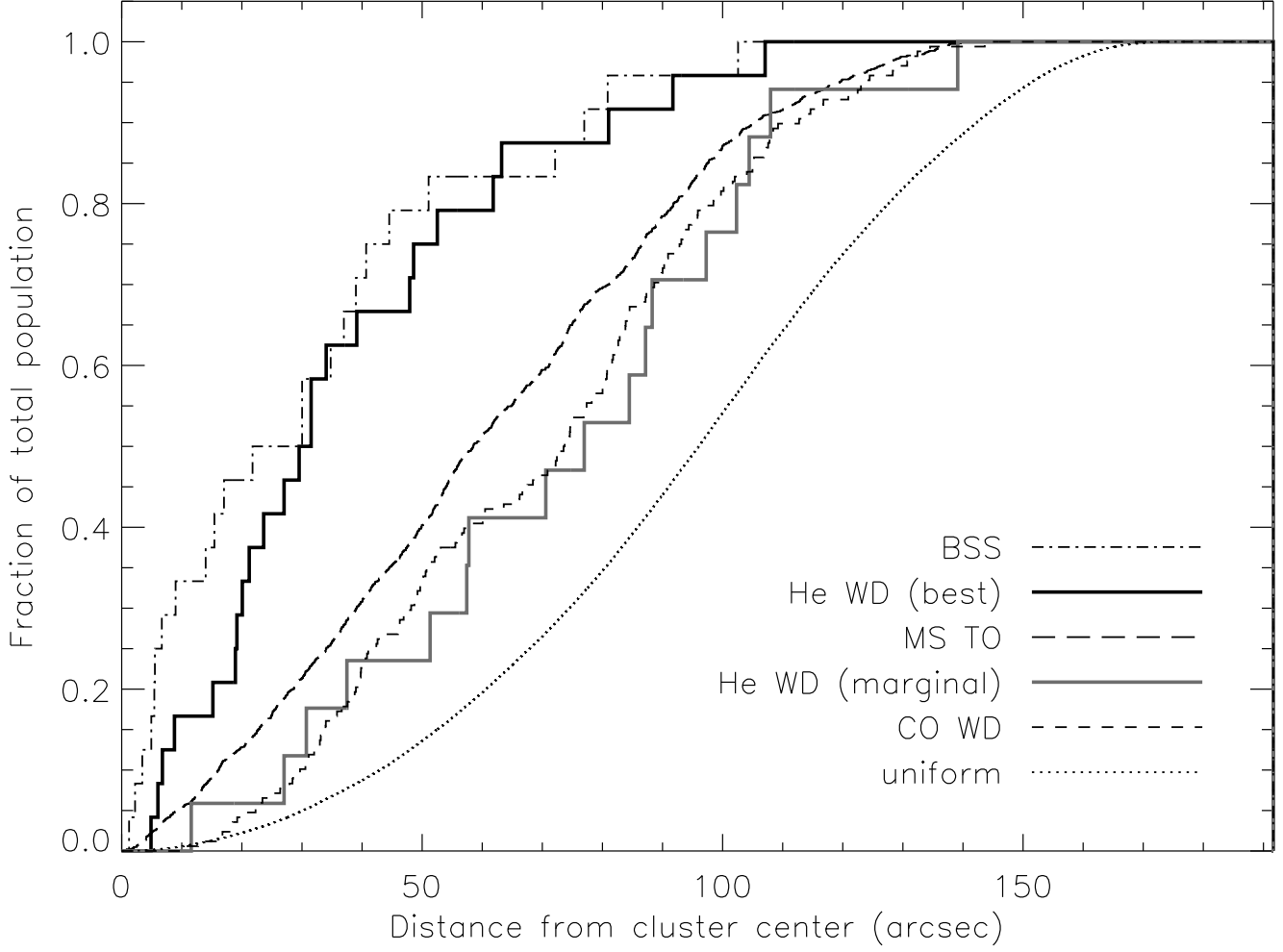


FIG. 5.— Cumulative radial distributions of various populations of stars in NGC 6397 and for a hypothetical uniformly distributed population. These distributions are used for the Kolmogorov-Smirnov tests described in the text (see §6.1). The dark solid line shows the distribution of the 24 best He WD candidates; the solid grey line is for the 17 marginal candidates. These can be compared with the distribution expected if the stars were unrelated to the cluster (dotted line) and with the distributions of 168 CO WDs (short-dash line), 1416 turnoff stars (long-dash line), and 24 blue stragglers (dash-dot line).

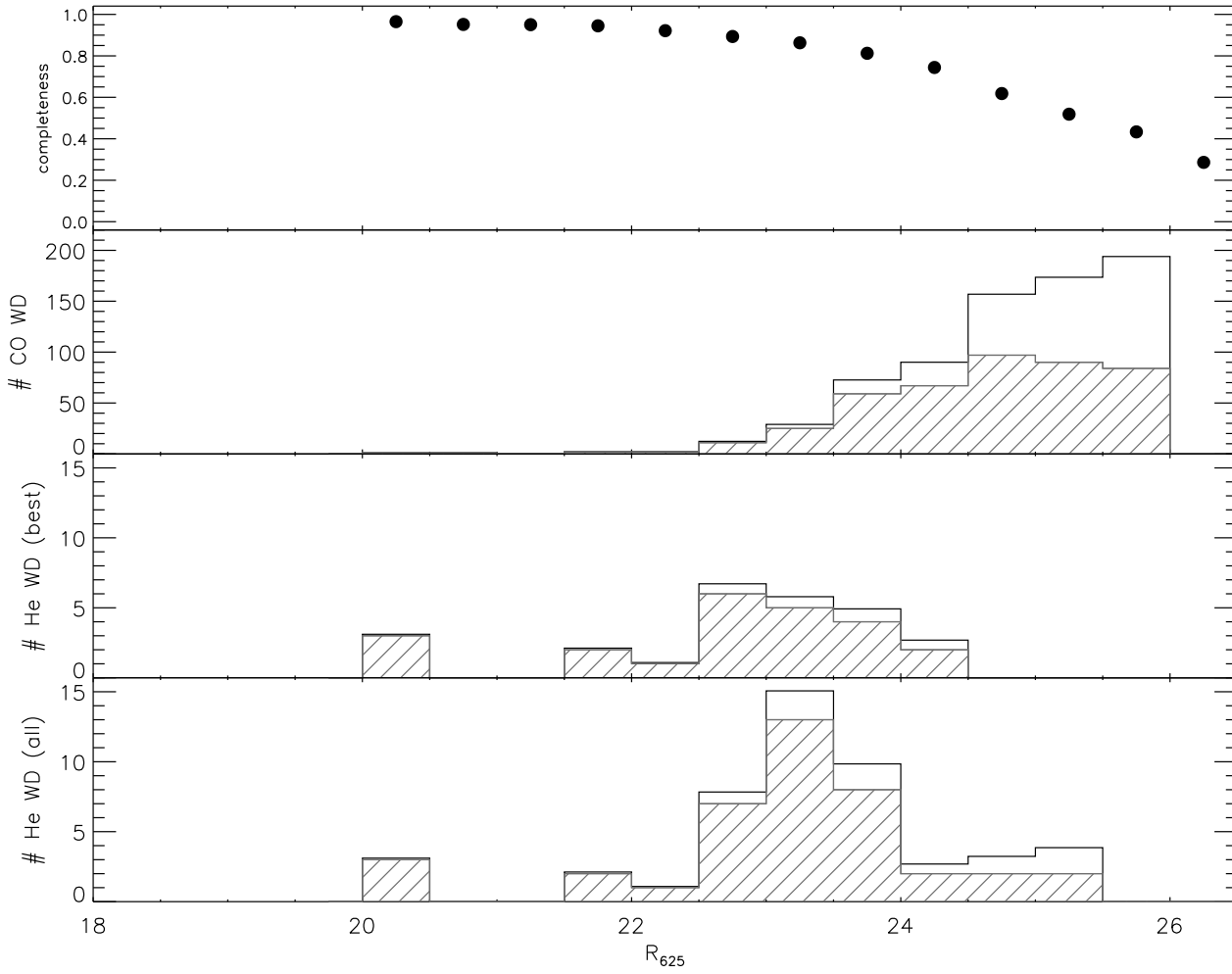


FIG. 6.— Results of artificial star tests. The top panel shows the fraction of stars recovered in artificial star tests for stars on the WD sequence as a function of R_{625} magnitude. We used these completeness statistics to infer the numbers of CO WDs (panel 2) and He WDs (best 24 only: panel 3; all: panel 4) in the cluster down to $R_{625} = 26$. Shaded histograms indicate numbers observed; white histograms include the completeness corrections. From the two bottom panels we conclude that, in contrast to the CO WD sequence, the He WD sequence ends before the magnitude limit is reached.

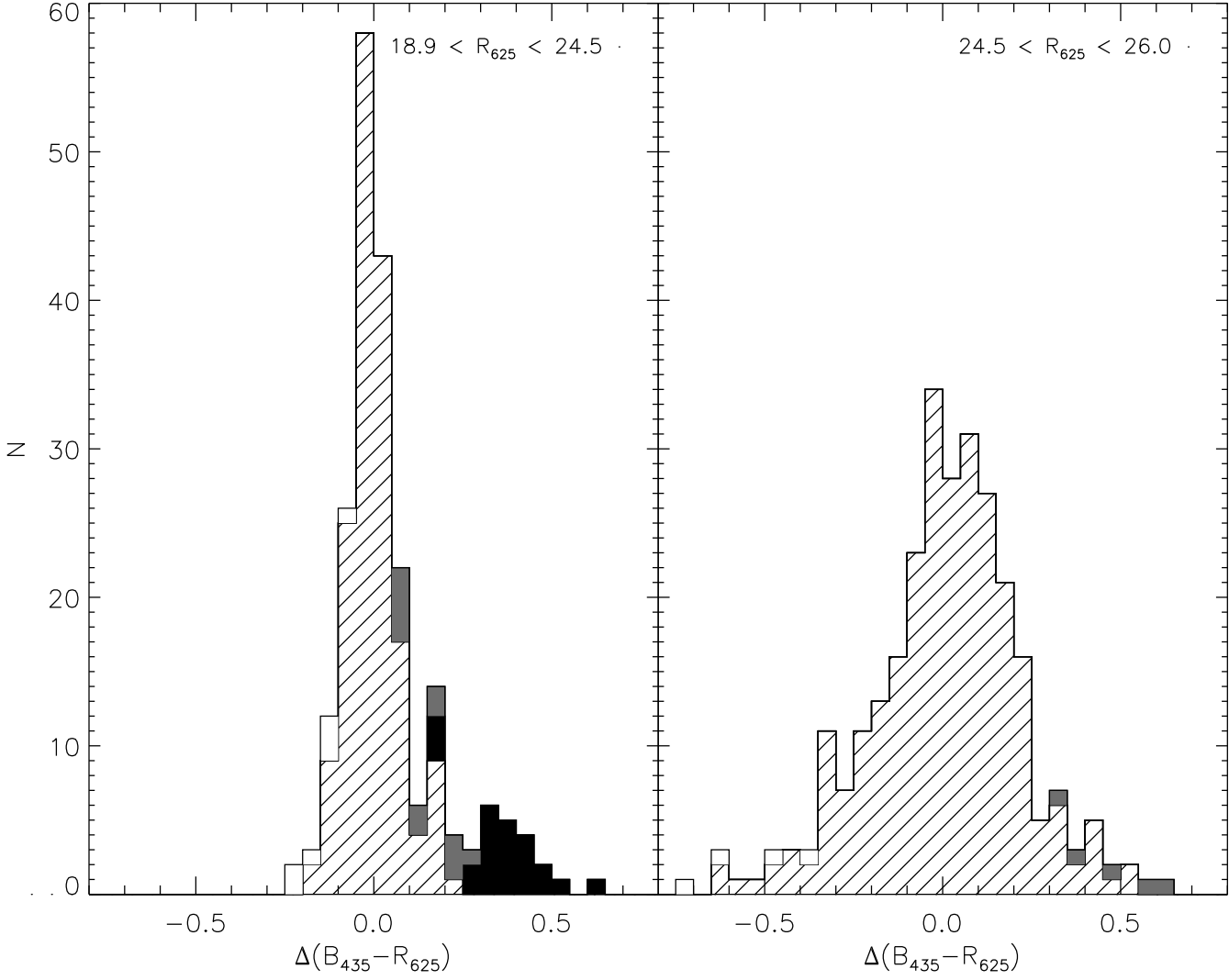


FIG. 7.— Color distribution of CO WDs and He WD candidates, measured relative to the color of the CO WD cooling track shown in Fig. 3. The left panel shows stars with $18.9 \leq R_{625} < 24.5$; the right panel shows stars with $24.5 \leq R_{625} < 26$. Diagonal-line shading denotes CO WDs. The best He WD candidates are shown in black and the marginal candidates in grey. Stars not assigned to either class are white. Among the brighter stars (left panel) the distribution is bimodal, with the He WDs forming a distinct second peak. At fainter magnitudes (right panel), the broadening of the CO WD sequence due to increased measurement uncertainties makes it more difficult to discern He WDs. However, there is no sign of any excess of stars on the right side as compared to the left.

TABLE 1
HELIUM-CORE WHITE DWARF CANDIDATES.

ID	x, y	R.A.	Dec.	Δr^1	R_{625}	$B_{435}-R_{625}$	$H\alpha-R_{625}$
1 ²	3147, 2683	17 40 40.659	-53 40 19.85	15.21	18.98	0.10	-0.04
2 ²	3073, 2540	17 40 41.076	-53 40 26.98	8.82	20.12	0.06	-0.03
3 ²	2780, 2529	17 40 42.722	-53 40 27.53	6.09	20.21	0.13	0.02
4	3208, 2146	17 40 40.314	-53 40 46.68	23.66	20.24	-0.01	-0.02
5	2511, 3382	17 40 44.237	-53 39 44.89	47.96	21.84	0.30	0.20
6	1650, 1160	17 40 49.083	-53 41 35.97	91.79	21.98	0.20	0.12
7	2349, 3401	17 40 45.145	-53 39 43.95	52.55	22.16	0.33	0.17
8 ³	2872, 3046	17 40 42.206	-53 40 01.67	27.09	22.53	0.56	0.15
9	1646, 2328	17 40 49.103	-53 40 37.57	63.29	22.59	0.20	0.25
10 ³	2942, 2417	17 40 41.813	-53 40 33.16	4.91	22.76	0.43	0.25
11	2383, 2868	17 40 44.957	-53 40 10.57	31.58	22.60	0.22	0.17
12	2219, 2489	17 40 45.882	-53 40 29.56	34.07	22.84	0.70	0.18
13	3391, 2834	17 40 39.285	-53 40 12.30	29.55	22.99	0.61	0.34
14	4980, 1989	17 40 30.344	-53 40 54.51	107.14	23.02	0.49	-0.19
15 ³	2875, 2371	17 40 42.189	-53 40 35.45	6.84	23.19	0.67	0.02
16	2652, 2823	17 40 43.444	-53 40 12.84	20.14	23.28	0.61	0.11
17	2940, 2128	17 40 41.823	-53 40 47.57	18.96	23.36	0.64	0.03
18	1639, 1485	17 40 49.144	-53 41 19.72	81.08	23.39	0.65	0.08
19	2481, 2430	17 40 44.406	-53 40 32.52	21.28	23.51	0.66	0.45
20	2182, 3162	17 40 46.085	-53 39 55.91	48.61	23.65	0.64	-0.02
21	2449, 1352	17 40 44.585	-53 41 26.38	61.90	23.72	0.68	0.15
22	2912, 2122	17 40 41.982	-53 40 47.92	19.20	23.75	0.77	0.07
23	3529, 2567	17 40 38.511	-53 40 25.63	31.59	24.07	0.85	0.34
24	3668, 2656	17 40 37.725	-53 40 21.17	39.16	24.22	0.83	-0.10
25	1810, 2869	17 40 48.183	-53 40 10.54	57.46	22.52	0.14	0.20
26	2852, 2278	17 40 42.317	-53 40 40.10	11.62	23.01	0.24	0.35
27	1447, 3511	17 40 50.218	-53 39 38.42	88.33	23.03	0.21	0.14
28	1174, 4690	17 40 51.751	-53 38 39.49	139.17	23.12	0.33	0.17
29	3404, 2152	17 40 39.212	-53 40 46.39	30.78	23.14	0.27	0.16
30	1885, 2663	17 40 47.760	-53 40 20.84	51.35	23.15	0.26	0.36
31	4196, 4234	17 40 34.759	-53 39 02.31	108.01	23.36	0.30	0.16
32	2190, 2749	17 40 46.045	-53 40 16.54	37.54	23.42	0.41	0.32
33	2511, 1147	17 40 44.239	-53 41 36.63	70.64	23.49	0.35	0.28
34	3363, 2786	17 40 39.443	-53 40 14.70	27.07	23.51	0.47	0.35
35	4813, 3345	17 40 31.287	-53 39 46.71	104.46	23.55	0.51	0.23
36	2762, 4447	17 40 42.825	-53 38 51.65	97.32	23.64	0.55	0.30
37	1529, 4027	17 40 49.758	-53 39 12.65	102.38	23.86	0.66	0.04
38	4275, 3578	17 40 34.314	-53 39 35.07	87.20	24.56	1.04	0.48
39	1899, 1926	17 40 47.683	-53 40 57.70	57.83	24.80	1.01	-0.21
40	2333, 3938	17 40 45.236	-53 39 17.07	77.05	25.31	1.44	-0.05
41	3438, 903	17 40 39.021	-53 41 48.85	84.52	25.50	1.44	0.93

¹ Offset in arcseconds from the cluster center. For the center we adopted $17^{\text{h}} 40^{\text{m}} 42^{\text{s}}.049$, $-53^{\circ} 40' 28''.72$ from Sosin (1997), which corresponds to $(x, y) = (2900, 2506)$ in the mosaic.

² ID=1, 2, and 3 correspond to NF1, NF2, and NF3 identified by Cool et al. (1998), respectively.

³ ID=8, 10, and 15 correspond to PC4, PC5, and PC6 identified by Taylor et al. (2001), respectively.

REFERENCES

- Anderson, S. F., Margon, B., Deutsch, E. W., & Downes, R. A. 1993, *AJ*, 106, 1049
- Anderson, S. F., Margon, B., Deutsch, E. W., Downes, R. A., & Allen, R. G. 1997, *ApJ*, 482, L69
- Anderson, J. & King, I. R. 2000, *PASP*, 112, 1360
- Anderson, J. & King, I. R. 2006, PSFs, Photometry, and Astrometry for the ACS/WFC. (Instrum. Sci. Rep ACS 2006-01; Baltimore: STScI)
- Anderson, J. et al. 2008, *AJ*, 135, 2055
- Anthony-Twarog, B. J., & Twarog, B. A. 2000, *AJ*, 120, 3111
- Anthony-Twarog, B. J., Twarog, B. A., & Suntzeff, N. B. 1992, *AJ*, 103, 1264
- Aurière, M., Lauzeral, C., & Ortolani, S. 1990, *Nature*, 344, 638
- Benacquista, M. J., 2006, *Living Rev. Relativity* 9, <http://www.livingreviews.org/lrr-2006-2>
- Bergeron, P., Wesemael, F., & Beauchamp A. 1995, *PASP*, 107, 1047
- Bogdanov, S., Grindlay, J. E., Heinke, C. O., Camilo, F., Freire, P. C. C., & Becker, W. 2006, *ApJ*, 646, 1104
- Calamida, A. et al. 2008, *ApJ*, 673, L29
- Castellani, M., & Castellani, V. 1993, *ApJ*, 407, 649
- Cohn, H. N., et al. 2009, in preparation
- Cool, A. M., and Bolton A. S. 2002, in *Stellar Collisions, Mergers and their Consequences*, ASP Conf. Series 263, ed. M. M. Shara (San Francisco: A.S.P.), 163
- Cool, A. M., Grindlay, J. E., Cohn, H. N., Lugger, P. M., & Slavin, S. D. 1995, *ApJ*, 439, 695
- Cool, A. M., Grindlay, J. E., Cohn, H. N., Lugger, P. M., & Bailyn, C. D. 1998, *ApJ*, 508, L75
- Cool, A. M., Piotto, G., & King, I. R. 1996, *ApJ*, 468, 655
- D'Amico, N., Possenti, A., Manchester, R. N., Sarkissian, J., Lyne, A. G., & Camilo, F. 2001, *ApJ*, 561, L89
- Davies, M. B., Benz, W., & Hills, J. G. 1991, *ApJ*, 381, 449
- Davis, D. S. et al. 2008, *MNRAS*, 383, L20
- De Marco, O., Shara, M. M., Zurek, D., Ouellette, J. A., Lanz, T., Saffer, R. A., & Sepinsky, J. F. 2005, *ApJ*, 632, 894
- Dieball A., Knigge C., Zurek, D. R., Shara, M. M., Long, K. S., Charles, P. A., Hannikainen, D. C., & van Zyl, L. 2005, *ApJ*, 634, L105
- Dotter, A., Chaboyer, B., Jevremovic, D., Kostov, V., Baron, E., & Ferguson, J. W. 2008, *ApJS*, 178, 89
- Dull, J. 1996, Ph.D. thesis, Indiana Univ.
- Edmonds, P. D., Gilliland, R. L., Heinke, C. O., Grindlay, J. E., & Camilo, F. 2001, *ApJ*, 557, L57
- Edmonds, P. D., Grindlay, J. E., Cool, A. M., Cohn, H. N., Lugger, P. M., & Bailyn, C. D. 1999, *ApJ*, 516, 250
- Ferraro, F. R., Possenti, A., Sabbi, E., & D'Amico, N. 2003, *ApJ*, 596, L211
- Gratton, R. G., Bragaglia, A., Carretta, E., Clementini, G., Desidera, S., Grundahl, F., & Lucatello S. 2003, *A&A*, 408, 529
- Grindlay, J. E., Cool, A. M., Callanan, P. J., Bailyn, C. D., Cohn, H. N., & Lugger, P. M., 1995, *ApJ*, 455, L47
- Grindlay, J. E., Heinke, C. O., Edmonds, P. D., Murray, S. S., & Cool, A. M. 2001, *ApJ*, 563, L53
- Hansen, B. M. S., Kalogera, V., & Rasio, F. A. 2003, *ApJ*, 586, 1364
- Hansen, B. M. S. et al. 2004, *ApJ*, 155, 551
- Hansen, B. M. S. et al. 2007, *ApJ*, 671, 380
- Harris, W. E. 1996, *AJ*, 112, 1487, <http://physwww.physics.mcmaster.ca/~harris/mwgc.dat>
- Hurley, J. R. & Shara, M. M. 2003, *ApJ*, 589, 179
- Hut, P. et al. 1992, *PASP*, 104, 981
- Ivanova, N., Heinke, C. O., Rasio, F. A., Taam, R. E., Belczynski, K., & Fregeau, J. 2006, *MNRAS*, 372, 1043
- Kalirai, J. S., Richer, H. B., Hansen, B. M. S., Reitzel, D., & Rich, R. M. 2005, *ApJ*, 618, L129
- King, I. R., Sosin, C., & Cool, A. M. 1995, *ApJ*, 452, L33
- Knigge, C., Dieball, A., Apellániz, J. M., Long, K. S., Zurek, D. R., & Shara, M. M. 2008, *ApJ*, 683, 1006
- Lauzeral, C., Ortolani, S., Aurière, M., & Melnick, G. 1992, *A&A*, 262, 63
- Liebert, J., Wesemael, F., Hansen, C. J., Fontaine, G., Shipman, H. L., Sion, E. M., Winget, D. E., & Green, R. F. 1986, *ApJ*, 309, 241
- Lopez, L. I. & Cool, A. M. 2007, *BAAS*, 210, 1605L
- Lugger, P. M., Cohn, H. N., & Grindlay, J. E. 1995, *ApJ*, 439, 191
- Marsh, T. R., Dhillon, V. S., & Duck, S. R. 1995, *MNRAS*, 275, 828
- Maxted, P. F. L., Marsh, T. R., & Moran, C. K. J. 2002, *MNRAS*, 332, 745
- Moehler, S. & Bono, G. 2008, *White Dwarfs*, eds. M. Burleigh & R. Napiwotzki (Springer Verlag, ASSL), in press (astro-ph/0806.4456v2)
- Moehler, S., Heber, U., Napiwotzki, R., Koester, D., & Renzini, A. 2000, *A&A*, 354, L75
- Moehler, S., Koester, D., Zoccali, M., Ferraro, F. R., Heber, U., Napiwotzki, R., & Renzini, A. 2000, *A&A*, 420, 515
- Nelemans, G., Yungelson, L. R., Portegies Zwart, S. F., & Verbunt, F. 2001a, *A&A*, 365, 491
- Nelemans, G., Portegies Zwart, S. F., Verbunt, F., & Yungelson, L. R. 2001b, *A&A*, 368, 939
- Nelemans, G., Jonker, P. G., & Steeghs, D. 2006, *MNRAS*, 370, 255
- O'Toole, S. J., Napiwotzki, R., Heber, U., Drechsel, H., Frandsen, S., Grundahl, F., & Bruntt, H. 2005, *Baltic Astronomy*, 15, 61
- Pols, O. R., Schröder, K-P., Hurley, J. R., Tout, C. A., & Eggleton, P. P. 1998, *MNRAS*, 298, 525
- Pretorius, M. L., Knigge, C., O'Donoghue, D., Henry, J. P., Gioia, I. M., & Mullis, C. R. 2007, *MNRAS*, 382, 1279
- Rappaport, S., Podsiadlowski, Ph., Joss, P. C., Di Stefano, R., & Han, Z. 1995, *MNRAS*, 273, 731
- Reid, I. N. 1998, *AJ*, 115, 204
- Renzini, A., et al. 1996, *ApJ*, 465, L23
- Richer, H. B., et al. 1997, *ApJ*, 484, 741
- Richer, H. B., et al. 2008, *ApJ*, 135, 2141
- Rohrmann, R. D., Serenelli, A. M., Althaus, L. G., & Benvenuto, O. G. 2002, *MNRAS*, 335, 499
- Saffer, R. A., Sepinski, J. F., De Marchi, G., Livio, M., Paresce, F., Shara, M., & Zurek, D. 2002, in *Stellar Collisions, Mergers and their Consequences*, ASP Conf. Series 263, ed. M. M. Shara (San Francisco: A.S.P.), 157
- Seaton, M. J. 1979, *MNRAS*, 187, 73P
- Serenelli, A. M., Althaus, L. G., Rohrmann, R. D., & Benvenuto, O. G. 2002, *MNRAS*, 337, 1091
- Sigurdsson, S., Richer, H. B., Hansen, B. M., Stairs, I. H., & Thorsett, S. E. 2003, *Science*, 301, 193
- Sirianni, M., et al. 2005, *PASP*, 117, 1049
- Sosin, C. A. 1997, Ph.D. thesis, Univ. California, Berkeley
- Stetson, P. B. 1987, *PASP*, 99, 191
- Stetson, P. B. 1994, *PASP*, 106, 250
- Strickler, R. R. 2008, Master's thesis, San Francisco State University
- Taylor, J. M., Grindlay, J. E., Edmonds, P. D., & Cool, A. M. 2001, *ApJ*, 553, L169
- Townsley, D. M., & Bildsten, L. 2002, *ApJ*, 565, L35
- Trager, S. C., King, I. R., & Djorgovski, S. 1995, *AJ*, 109, 218
- Tremblay, P. E., & Bergeron, P. 2008, *ApJ*, 672, 1144
- van Kerwijk, M. H., Bassa, C. G., Jacoby, B. A., & Jonker, P. G. 2005, in *Binary Radio Pulsars*, ASP Conf. Series 328, eds. F. A. Rasio and I. H. Stairs (San Francisco: A.S.P.), 357
- Verbunt, F., Bunk, W. H., Ritter, H., & Pfeffermann, E. 1997, *A&A*, 327, 602
- Webbink, R. F. 1975, *MNRAS*, 171, 555
- Williams, G. 1983, *ApJS*, 53, 523
- Zoccali, M., et al. 2001, *ApJ*, 553, 733